ENHANCEMENT OF CYANOBACTERIAL GROWTH BY RIVERINE PARTICULATE MATERIAL

Christian Grimm[a,*], Raul E. Martinez[b†], Oleg S. Pokrovsky[a,c,d], Liane G. Benning[e,f], and Eric H. Oelkers[a,g]

[a]GET, CNRS/URM 5563, Université Paul-Sabatier, 14 Ave Edouard-Belin, 31400 Toulouse, France.

[b]Geo- und Umweltnaturwissenschaften, Albert-Ludwigs Universität, 79104 Freiburg, Germany.

[c]N. Laverov Federal Center of Integrated Arctic Research, Russian Academy of Science, Arkhangelsk, Russia.

[d]BIO-GEO-CLIM Laboratory, Tomsk State University, 634050 Tomsk, Russia

[e]School of Earth and Environment, University of Leeds, LS2 9JT, UK.

[f]GFZ German Research Centre for Geosciences, 14473 Potsdam, Germany.

[g]Earth Sciences, University College London, Gower Street London WC1E 6BT, UK.

*Corresponding author: Christian Grimm (christian-grimm@gmx.de)

†Current address: Max-Planck-Research Group Paleobiogeochemistry, University of Bremen, Am Biologischen Garten 2, 28359 Bremen, Germany.

Abstract

Particulate material plays a major role in the transport of sparingly soluble nutrients such as P and Fe in natural surface waters. Microbes might gain access to these nutrients either indirectly through particulate dissolution or directly through microbial attack. As such, it seems reasonable to expect a link between the particulate material concentration and bacterial growth in natural surface waters. To explore this link, a series of microcosm growth experiments were performed with a typical freshwater cyanobacteria *Synechococcus sp.* grown in dilute BG-11 culture media in the presence and absence of basaltic and continental riverine particulate material. Results demonstrate that riverine particulates can increase bacterial biomass by 1) triggering bacterial growth in otherwise unfavourable conditions, 2) increasing total maximum biomass concentration, and 3) inducing bacteria growth during the post-exponential phase. These effects are found to be enhanced by increasing particulate concentration. Results also indicate a positive feedback between the nutrient release from the particulates and growing bacteria, where dissolving particulates enhance bacterial growth,

which further promotes particulate dissolution by altering fluid pH. Microscopic analysis showed direct physical contact between particulates and cyanobacteria, suggesting that bacteria attach directly on mineral surfaces to gain required nutrients. Furthermore, frequent bacteria clusters were observed associated with particulates, indicating an increasing aggregation of bacteria in the presence of particulate material, which may facilitate a higher burial efficiency of organic carbon.

Keywords: CO_2, cyanobacteria, organic carbon cycle, primary production, riverine particulate material, nutrients

1 Introduction

Atmospheric CO_2 concentrations have been steadily increasing since the beginning of the industrial revolution and there is exhaustive research linking it to global climate change. Carbon dioxide is removed from the atmosphere by two major mechanisms: The 'inorganic pathway', which couples the dissolution of divalent metal bearing silicate minerals to the formation of carbonate minerals and the 'organic pathway', which removes CO_2 from the atmosphere by photosynthesis and the subsequent burial of organic matter (Berner, 1982; Berner et al., 1983; Berner and Kothavala, 2001; Falkowski et al., 1998; Gislason et al., 2009; Walker et al., 1981; Wallmann, 2001). Burial of organic matter is required for the long-term drawdown of CO_2 via the 'organic pathway' because it prevents organic matter decomposition and thus the return of CO_2 to the atmosphere (Berner, 1982; Falkowski et al., 1998; Jeandel and Oelkers, 2015). Besides CO_2 and light, photosynthesizing microorganisms require nutrients for their metabolic activity. A lack of nutrients, such as P, N, Si, or Fe can be the limiting factor for primary production (Broecker, 1982; Falkowski et al., 1998; Jickells et al., 2005; Mills et al., 2004), whereas in turbid environments, light can limit bacterial growth (Anderson et al., 2002). The two major sources of nutrients to natural surface waters are the recycling of organic compounds due to microbial degradation and the influx of new nutrients through rivers, aeolian dust or volcanic ash (Eiriksdottir et al., 2015; Eiriksdottir, 2016; Falkowski, 2014; Jickells et al., 2005; Jones and Gislason, 2008; Olsson et al., 2013).

Rivers carry elements derived from continental weathering in dissolved and particulate form. Whereas the dissolved riverine transport has received much greater interest in the past, recent estimates of riverine particulate fluxes concluded that the suspended material flux dominates the dissolved flux for essentially all elements, except for the most soluble like Na (Gislason et al., 2006; Jeandel and Oelkers, 2015; Jones et al., 2012; Oelkers et al., 2011;

2012). The estimated global dissolved riverine flux is approximately 1 Gt year^{-1} (Gaillardet et al., 1999; 2003; Meybeck et al., 2003; Viers et al., 2009), whereas the suspended particulate land-to-ocean flux is estimated to be 15-20 Gt year^{-1}, thus at least an order of magnitude greater (Meybeck et al., 2003; Oelkers et al., 2011; Syvitski et al., 2003; Walling, 2006). Including the estimated bedload component of 1.6 to 10 Gt year^{-1}, the total particulate flux exceeds the dissolved flux by a factor of 17 to 30 (Jeandel and Oelkers, 2015; Walling, 2006). The predominance of particulate over dissolved transport at a global scale is depicted in Figure 1 for a selection of vital and often limiting nutrients. For example, the riverine particulate flux of Si, P and Fe exceeds the corresponding dissolved flux by factors of 50, 100 and 350, respectively (Jeandel and Oelkers, 2015; Oelkers et al., 2011). Moreover, much of what is commonly measured as dissolved flux may in fact be present as colloids and nanoparticles (Gaillardet et al., 2003).

Jeandel and Oelkers (2015) summarized the potential role of riverine particulate material in the burial and preservation of organic carbon. First, an increasing supply of particulate material accelerates the sediment accumulation rate, thus reducing organic material exposure time to oxygen and the organic matter decomposition. Secondly, the supply of mineral surfaces is viewed as major control of organic matter burial due to strong organic material sorption onto

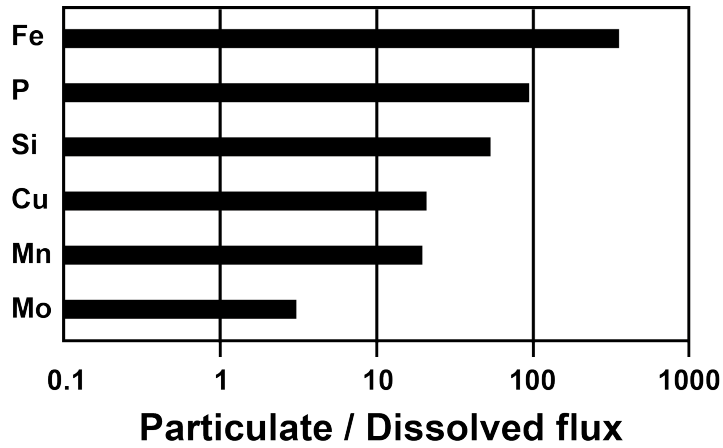

Figure 1. The ratio of global riverine particulate flux to the corresponding dissolved flux for selected nutrients. Particulate fluxes of the vital nutrients Si, P and Fe exceed the corresponding dissolved fluxes by factors of 50, 100 and 350. Figure modified after Oelkers et al. (2011).

mineral grains (Burdige, 2007; Kennedy et al., 2002; Lalonde et al., 2012; Mayer, 1994). Note also, that riverine particulate transport in the global rivers is particularly climate sensitive (Gislason et al., 2009; Jeandel and Oelkers, 2015). An increasing CO_2 concentration in the

atmosphere leads to higher air temperatures, changing precipitations patterns and increasing runoff, which leads to elevated chemical and physical weathering rates (Alley et al., 1997; Gedney et al., 2006; Gislason et al., 2006; 2009; Labat et al., 2004). The increasing weathering rates in turn drive the CO_2 drawdown via both the 'inorganic' and 'organic pathway' through the delivery of divalent cations as well as limiting nutrients.

The significance of terrestrial sediments on bacterial productivity has received some attention, notably due to their potential source of bio-available Fe. The dissolution of Fe in continental shelf sediments has been attributed as major source of dissolved Fe to the oceans (Dale et al., 2015; Elrod et al., 2004; Jeandel and Oelkers, 2015; Jones et al., 2011; Radic et al., 2011). However, the direct effect of riverine particulates on bacterial growth has not been investigated in detail. Direct and indirect interactions between minerals and microbes, however, are common or even omnipresent in natural systems. For example, Bailey et al. (2009) demonstrated, in an experimental study, the capability of microbes to obtain required nutrients directly from basaltic glass. Similarly, Rogers et al. (1998) and Rogers and Bennett (2004) showed in a field and experimental study that P-bearing silicates were heavily colonized and weathered by subsurface microorganisms, whereas P-free silicates were not. They concluded that microorganisms acquired inorganic P directly from the silicate minerals. More recently, Sudek et al. (2017) observed elevated growth rates of the heterotrophic bacterium *Pseudomonas stutzeri VS-10* in the presence of basaltic glass and concluded that the physical contact between the bacterium and the glass is critical in this process. Perez et al. (2016) described elevated growth rates of the heterotrophic bacterium *Pseudomonas aeruginosa* in the presence of Fe-bearing basaltic glass compared to Fe-free basalts and control experiments without basalt.

Microorganisms have been shown to influence mineral dissolution and precipitation reactions. For example in lacustrine settings, the growth of cyanobacteria has been demonstrated to catalyze calcium carbonate formation through the creation of an alkaline growth environment around the cell (Dittrich et al., 2003; Hodell et al., 1998; Lee et al., 2006; Stabel, 1986; Thompson et al., 1997). In addition, microorganisms can accelerate the dissolution of a variety of silicate minerals through their effect on pH, or through microbially produced organic ligands that either form complex aqueous metals or Si-framework destabilizing surface complexes (Bennett et al., 2001; Drever and Stillings, 1997; Olsson-Francis et al., 2012; Perez et al., 2016; Rogers and Bennett, 2004; Stockmann et al., 2012; Uroz et al., 2009; Wu et al., 2007; 2008). Notably, when directly attached to mineral surfaces,

microorganisms can alter Si-solubility by perturbing mineral-water equilibria in their microenvironment (Rogers and Bennett, 2004). It is a matter of discussion, however, whether this interaction is the coincidental effect of the microbial metabolism, or an active strategy of the microorganisms to get access to vital nutrients directly from the rocks (Bennett et al., 2001).

The interactions of microbes and minerals described above, together with the vast source of nutrients present in riverine particulates, suggest an influence of riverine particulate material on bacterial growth in natural environments. This study aims to explore the effect of riverine particulate material on the growth of freshwater cyanobacteria. Towards this goal, we conducted microcosm growth experiments with the freshwater cyanobacteria *Synechococcus sp.*, a common planktonic cyanobacterium, in the presence and absence of two types of riverine particulate material. Further experiments were run in an attempt to identify the factors leading to the bacterial growth enhancement in the presence of these particles. The purpose of this paper is to present the results of this experimental study and to use these results to assess the potential role of riverine particulates on microbial growth in natural systems.

2 Materials

2.1 Riverine Particulate Material

Two different types of riverine particulate material (RPM) with distinct chemical and mineralogical compositions were used in this study to quantify their presence on cyanobacteria growth. The bulk chemical compositions as well as the BET (Brunauer, Emmett and Teller, 1938) surface areas of these particulates are listed in Table 1. One additional experiment was run in the presence of zircon particles, to evaluate the effect of the presence of inert mineral surfaces on growth. The riverine particulates used in this study were:

1) **MS**, bedload material from the Mississippi river collected in July 2010 in western New Orleans, USA. This sample is described in detail in Jones et al. (2012) where its chemical composition and its BET surface area were reported. The Mississippi RPM consists of almost 80% SiO_2 and is mainly composed of quartz and feldspars with minor concentrations of sheet silicates. It was chosen as representative of continental riverine material. The XRD spectrum of this sample, provided in Figure A1, shows a smooth pattern with well localized peaks, which can almost be perfectly fit assuming the sample contained only quartz and feldspar.

2) **ICE**, suspended basaltic particulates collected from the Jökulsá á Fjöllum, a glacial river in Eastern Iceland. The major chemical components of this Iceland RPM are 51.5 % SiO_2, 13.6 % Al_2O_3, 12.2 % FeO and 10.4 % CaO. It is mainly composed of basaltic glass and basalt fragments. The XRD spectrum, illustrated in Figure A1, shows a pattern typical for glassy material. The observed peaks can be best fit by a combination of plagioclase and pyroxene. This sample is representative of the high relief, volcanic and tectonic active islands that contribute over 45 % of river suspended material globally (Eiriksdottir et al., 2008; Milliman and Syvitski, 1992). Details on sampling and filtration methods can be found in Eiriksdottir et al. (2008), where the chemical composition of the sample was first reported (sample ID 01A033 therein).

2.2 Cyanobacteria

The unicellular freshwater cyanobacteria *Synechococcus sp. PCC 7942* used in this study were cultured under sterile conditions in 100% BG-11 Freshwater Solution Medium (Sigma-Aldrich C3061) at room temperature, 24 h illumination at 3000 LUX cool white fluorescence light and bubbling of humidified air to achieve constant mixing. *Synechococcus* were chosen for this study because of their great abundance in freshwater and marine environments (Obst et al., 2009a, b). The cyanobacteria *Synechococcus sp*. and *Prochlorococcus sp*. are responsible for >25 % of global photosynthesis (Rohwer and Thurber, 2009). Further details about this cyanobacteria are provided in Dittrich and Sibler (2006), Obst et al. (2009a), Obst et al. (2009b) and Bundeleva et al. (2014). The initial cyanobacteria cultures showed minor heterotrophic cortege (<5 % of the biomass), as identified by agar plate counting of the stock solution.

Table 1. Whole rock analyses and specific surface areas of the riverine particulate material used in this study. Mississippi (MS) data is from Jones et al. (2012), Iceland (ICE) data from Eiriksdottir et al. (2008). Note that total Fe is presented as FeO or Fe_2O_3, respectively, for the ICE and MS samples.

Name	**ICE**	**MS**
Particulate type	suspended	Bedload
BET (m^2g^{-1})	8.92	3.05

SiO_2 (%)	51.54	79.25
Na_2O (%)	2.67	1.56
MgO (%)	5.86	0.51
Al_2O_3 (%)	13.62	6.38
P_2O_5 (%)	0.28	0.10
K_2O (%)	0.47	1.71
CaO (%)	10.44	1.34
TiO_2 (%)	2.52	0.43
MnO (%)	0.22	0.03
FeO (ICE) (%)	12.24	
Fe_2O_3 (MS) (%)		1.39

3 Methods

3.1 Growth Experiments

Synechococcus sp growth experiments were performed in sterile 250 and 500 ml Polycarbonate flasks with 12 h/12 h illumination/dark cycles (3000 LUX cool white fluorescence light during daytime), circular shaking at 250 cycles/min, and at a temperature of 21±2°C. Reactors were closed with BIO-SILICO© stoppers that allowed sterile equilibration with the atmosphere. The reactive fluids were composed of 1:1000 or 1:375 dilutions of the 50x concentrated BG-11 Freshwater Solution culture medium to obtain a 5 % and 13.3 % dilution of this BG-11 culture medium. These dilutions were adopted to limit the nutrient content originally present in our experiments, which were designed to assess the potential role of natural particulate material to provide essential nutrients for bacterial growth. The resulting chemical compositions of these diluted fluids are listed in Table 2. The majority of the experiments were began in the 5 % BG-11 media, whereas a few were began using the higher nutrient fluid. The riverine particulate material was cleaned and sterilized following different protocols, in part to determine if these treatments affected the experimental results and to remove any preexisting bacteria from the particulates. They were either sterilized overnight in the oven at 121 °C with or without previous ethanol rinsing, or sterilized by H_2O_2 treatment, or burned in the oven at 450 °C for 2.5 hours. Note, that these treatments potentially alter the particle surfaces distinctly, potentially creating more fresh inorganic sites, while reducing the number of reactive organic sites. Particulates were added to the reactors in concentrations ranging from 75 mg/kg to 1500 mg/kg, corresponding to a low and a high natural riverine particulate concentrations according to Meybeck et al. (2003). To determine the effect of particle liberated elements on cyanobacteria growth in the absence of the physical particles, several experiments were begun with a fluid that was created by first dissolving 1500 mg/kg MS or ICE RPM for one month in bacteria-free 5 % BG-11 media then subsequently filtered to separate the fluid from these particulates. Biotic control experiments were run in the

absence of RPM and abiotic control experiments were run in the presence of particulates but the absence of added cyanobacteria. All reactive fluids, as well as the experimental equipment were either filter-sterilized or autoclaved at 121 °C for 20 minutes prior to each experiment.

Aliquots of the bacteria stocks were harvested from the stationary growth stage and rinsed three times in the initial starting fluid for each experiment by centrifugation/resuspension cycles prior to inoculation. Inoculates were harvested 4-6 weeks after initial stock culturing in order to have similar proportions of dead cells and to add the same total quantity of fluid to all experiments. Cyanobacteria were inoculated into the experimental reactors in biomass concentrations ranging from 0.007, to 0.041 $g_{(dry)}$/kg. Table A1 reports the initial conditions of all experiments.

Table 2. Composition of BG-11 freshwater culture solution and its 5% and 13.33% dilutions used to perform the growth experiments in the present study. FAC stands for Ferric Ammonium Citrate. The BG-11 composition was taken from Rippka et al. (1979).

Salt	**Concentration (mmol/kg)** BG-11 dilution:		
	100%	**5%**	**13.33%**
$NaNO_3$	17.60	0.88	2.347
K_2HPO_4	0.23	1.15×10^{-2}	3.07×10^{-2}
$MgSO_4*7H_2O$	0.30	1.50×10^{-2}	4.00×10^{-2}
$CaCl_2*2H_2O$	0.24	1.20×10^{-2}	3.20×10^{-2}
Citric Acid*H_2O	0.031	1.55×10^{-3}	4.13×10^{-2}
FAC	0.021	1.05×10^{-3}	2.80×10^{-2}
$Na_2EDTA*2H_2O$	0.0027	1.35×10^{-4}	3.60×10^{-4}
Na_2CO_3	0.19	9.50×10^{-3}	2.53×10^{-2}
H_3BO_3	0.046	2.30×10^{-3}	6.13×10^{-3}
$MnCl_2*4H_2O$	0.009	4.50×10^{-4}	1.20×10^{-3}
$ZnSO_4*7H_2O$	0.00077	3.85×10^{-5}	1.03×10^{-4}
$Na_2MoO_4*2H_2O$	0.0016	8.00×10^{-5}	2.13×10^{-4}
$CuSO_4*5H_2O$	0.0003	1.50×10^{-5}	4.00×10^{-5}
$Co(NO_3)_2*6H_2O$	0.00017	8.50×10^{-6}	2.27×10^{-5}

3.2 Sampling

Aliquots of homogenous samples containing fluid, bacteria and particulates were periodically taken from each experiment in a sterile laminar hood box, 6h after the onset of illumination. Solids were thoroughly resuspended prior to sampling to preserve constant RPM and bacteria concentrations during each experiment. The sample volume was 3 ml from the 250 ml reactors, where only biomass and pH were measured, and 15 ml from 500 ml reactors, where the fluids were further analyzed for elemental composition, dissolved inorganic carbon (DIC) and non-purgeable organic carbon (NPOC). In selected experiments, solids sampled

230 during and after the experiment and prepared for SEM analysis. Optical density and pH were
231 measured on the homogeneous fluid, bacteria and particulate bearing samples immediately
232 after sampling, whilst fluid supernatants were filtered using a MilliPore 0.45 µm cellulose
233 acetate filter for further analyses.

234 *3.3 Analytical methods*

235 *3.3.1 Biomass concentration*

236 Biomass concentrations in the homogeneous fluid, bacteria, and particulate bearing
237 samples were determined from optical density (OD) measurements using a Varian
238 Cary50Scan Spectrophotometer. Optical density readings were then converted to dry biomass
239 using a linear calibration curve over the concentration range of the experiments. The
240 calibration curve (Figure A 2) was generated by plotting the measured ODs of five
241 cyanobacteria stock solutions of different concentrations against their corresponding dry
242 weights as determined gravimetrically. Measurements were done at the peak absorption of
243 chlorophyll a (682 nm) and the contribution of fluid turbidity (measured at 750 nm) was
244 subtracted from the 682 nm reading. This approach accounts for the contribution of riverine
245 particulates and/or cell debris on the OD measurements. As depicted in Figure 2A, the effect
246 of different particulate concentrations on optical density was accurately accounted for by the
247 difference of two wavelengths. Note the 682 nm peak shifts towards a lower wavelength when
248 cyanobacteria die, which gives an indication of their physical state. Abiotic fluids of each
249 particulate concentration were measured following the same protocol to correct for the effect
250 on OD (682-750 nm) of the presence of these particulates and to control for possible
251 contamination; measurements of the abiotic particulate bearing fluids were subtracted from
252 their corresponding biotic fluids. The optical density of each sample was measured in
253 triplicate and total uncertainty was estimated to be below 10 %.

254 To validate the OD measurement of biomass, chlorophyll *a* was measured via pigment
255 extraction in selected experimental fluids. These chlorophyll *a* analyses were performed by
256 first diluting a 0.3 ml suspension sample in a glass vial with 2.7 ml acetone to produce a 90 %
257 acetone solution. After storage for two days at -20 °C with occasional shaking, the samples
258 were centrifuged for 10 min at 4500 rpm and absorbance was measured with a
259 spectrophotometer at 750 nm, 663 nm, 645 nm and 633 nm. Chlorophyll *a* concentration was
260 then calculated using the SCOR-Unesco Report (1966) equation: chlorophyll *a* = 11.96 x
261 (663nm-750nm) - 2.16 x (645-750nm) + 0.1 x (630-750nm). Figure 2B shows the correlation
262 of the two different methods for biomass measurement in three experiments. The good

correlation (R^2 = 0.93) validates our biomass concentrations determinations using optical density measurements. Therefore, biomass concentration could be determined rapidly in a high number of samples without applying time consuming techniques such as described in Wojtasiewicz and Ston-Egiert (2016).

3.3.2 DIC/NPOC

Dissolved inorganic (DIC) and non-purgeable organic carbon (NPOC) were measured using a Shimadzu TOC-VCSN Carbon Analyzer with a ASI-V sample unit at the CNRS laboratory 'Géosciences Environnement Toulouse'. The detection limits were 0.57 ppm and 0.47 ppm for DIC and NPOC and the uncertainty below 3 %.

3.3.3 ICP-MS

The aqueous major and trace element concentrations were determined in fluids collected from several experiments by High Resolution Inductively Coupled Plasma Mass Spectrometry (HR-ICP-MS) using a Thermo-Finnigan Element-XR at the Géosciences Environnement Toulouse. Multi-element standard solutions were used for calibration. The analytical uncertainty of these measurements was below 2 %.

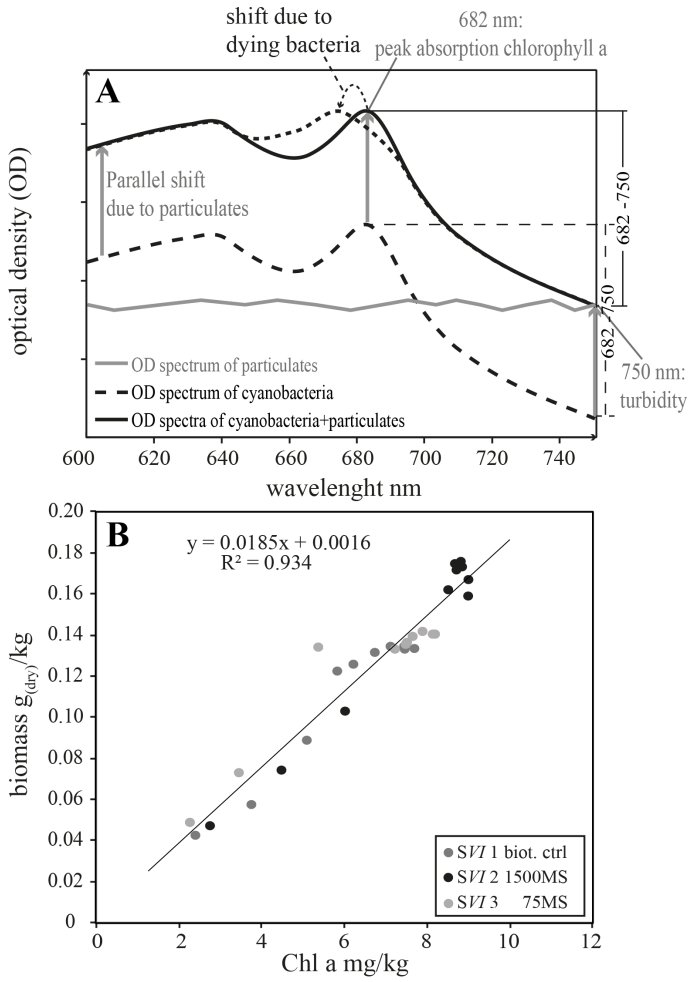

Figure 2. A: Spectrophotometric scan of representative cyanobacteria bearing reactive fluids with (solid black line) and without (dashed black line) particulates (grey line) from 600 to 750 nm. The presence of particulates shift the optical density curves to higher total values without changing the shape of the spectra over the 682 to 750 nm range. In the presence of dead cyanobacteria the difference in the absorbance between 682 to 750 nm decreases due to a shift of the absorption peak to lower wavelengths B: Correlation of measured biomass and chlorophyll *a* concentration in experiments where both were measured.

3.3.4 Scanning electron microscopy (SEM)

Solid samples (particulate-bacteria mixtures) were analyzed using a FEI Quanta 650 FEG-ESEM Scanning Electron Microscope (SEM) at the School of Earth and Environment at the University of Leeds. To avoid destruction of the bacteria in high vacuum, samples were previously fixed by Glutaraldehyde treatment as follows: The recovered particulate/bacteria mixtures were stored for one night in a sterile 2.5 % Glutaraldehyde solution (25 % stock solution diluted 1:10 in 50 mM Na_3PO_4) to preserve the bacteria. Subsequently, the samples were ethanol exchanged by suspending them in gradually increasing ethanol concentrations up to pure ethanol. Finally, samples were critical point dried using a Polaron E3000 CPD unit, mounted on sample stubs and gold coated prior to analysis.

3.4 Growth rates

The variation of biomass concentration over time in our experiments followed logistic bacterial growth equation, which can be expressed as (Ernst et al., 2005)

$$biomass\ concentration = \frac{a}{1+e^{-k(t-c)}} + a_0 \qquad (2)$$

where a represents the upper asymptote of the sigmoidal growth curve, a_0 reflects the initial biomass concentration, k stands for a rate parameter describing the rate at which growth initially accelerates and c designates a time constant describing the time elapsed between the beginning of the experiment and the turning point (point of maximal increase in biomass concentration). The variation of biomass concentrations consistent with this behavior is shown in Fig. 3. The logistic bacteria growth curve **Error! Reference source not found.**consists of an initial lag period, followed by an acceleration phase and an exponential growth phase, during which the growth rate is constant. After the exponential growth, rates decelerate until the culture enters the stationary phase during which little or no growth occurs.

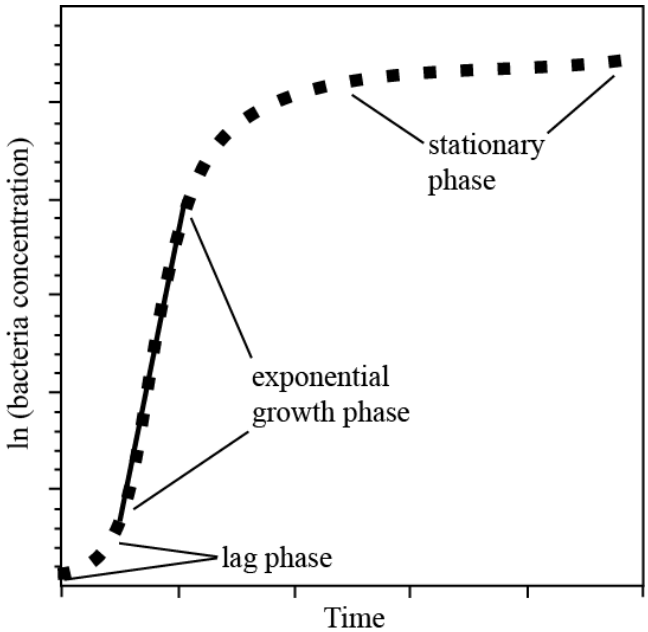

Figure 3. Typical logistic bacterial growth curve depicted as the logarithm of biomass concentration versus time. After an initial lag period, bacterial growth accelerates and reaches an exponential growth phase during which the growth rate is constant. After exponential growth, rates decelerate until the culture enters the stationary phase during which little or no growth occurs.

Bacterial growth rates in this study were calculated using the *GrowthRates* software (Version 2.1, December 11, 2015) developed by Barry G. Hall and others at the Bellingham Research Institute (Hall et al., 2014). The growth rate constant μ is calculated only considering the exponential growth phase according to:

$$\mu = \frac{(lnN_{t_2} - lnN_{t_1})}{(t_2 - t_1)} \qquad (1)$$

where N_t represents the biomass concentration at time t. The dimension of μ is reciprocal time. The results obtained from the *GrowthRates* program were verified by hand for each experiment. The uncertainty in the retrieved values of μ is given by the standard error of the linear regression of the biomass concentrations considered to calculate the rate. If only two points were used for the calculation, the uncertainties in μ are estimated to be ±20 % based on the associated uncertainties in the biomass concentrations. The bacterial growth behavior in the stationary phase was quantified by linear regression and is presented as the stationary phase growth rate, μ_{stat}.

4. Results

In total, 130 experiments were run. Table A 2 summarizes the observed maximum biomass concentration, the calculated growth rate constant μ, and the stationary phase growth rate μ_{stat} for all of these experiments. A detailed list of all measurements performed during each experiment can be found in the electronic supplement, including all biotic and abiotic controls. Among these experiments there were numerous duplicates, in each case the duplicate experiment provided results close to the originals. The results of some of representative experiments are presented and plotted in selected groups in the figures below to illustrate the effects of various factors on *Synechococcus sp.* growth rates. Table A1 and Table A **2** also list in which figure the results of an experiment are displayed. All experiments in which bacteria grew exhibited typical logistic bacterial growth. Differences were observed, however, depending on the presence or absence of Iceland and Mississippi riverine particulate material (RPM) as will be seen below.

4.1 Temporal evolution of biomass concentration in the presence and absence of Mississippi and Iceland RPM

Figure 4 shows the temporal evolution of biomass concentration of representative growth experiments in the presence and absence of 1500 mg/kg Mississippi (Figure 4A) and 1500 mg/kg Iceland (Figure 4B) riverine particulate material. These experiments were performed at an initial pH of 5.9, containing 5 % BG-11 media and a 0.018 $g_{(dry)}$/kg initial biomass concentration. The different colors in the figure correspond to different protocols of sterilization of the riverine particulate material. No bacterial growth was observed in the biotic control experiments; these experiments were performed by placing the 0.018 $g_{(dry)}$/kg initial biomass concentration into reactors with the same initial conditions as the other

experiments in these figures but in the absence of RPM. In contrast, *Synechococcus sp.* showed typical logistic growth to an average maximum biomass concentrations of 0.151±0.008 $g_{(dry)}$/kg and 0.151±0.012 $g_{(dry)}$/kg, in the presence of 1500 mg/kg MS and ICE RPM, respectively. The calculated growth rate constant μ during the exponential growth phase was 0.41±0.08 and 0.37±0.08 day^{-1} for 1500 mg/kg MS and ICE RPM bearing experiments, respectively. In the presence of MS RPM, the exponential growth was followed by a steady increase in biomass concentration during the stationary phase at an average rate, μ_{stat}= (8.4±2.2)×10^{-04} $g_{(dry)}$/kg/day. Note these rates correspond to the average and standard deviations of the four replicates run using the distinct sterilization protocols shown in the figure. In the presence of 1500 mg/kg ICE RPM, the bacteria concentration remained constant or slightly decreased during the stationary phase. Two experiments containing ICE RPM were stopped immediately after the exponential growth phase.

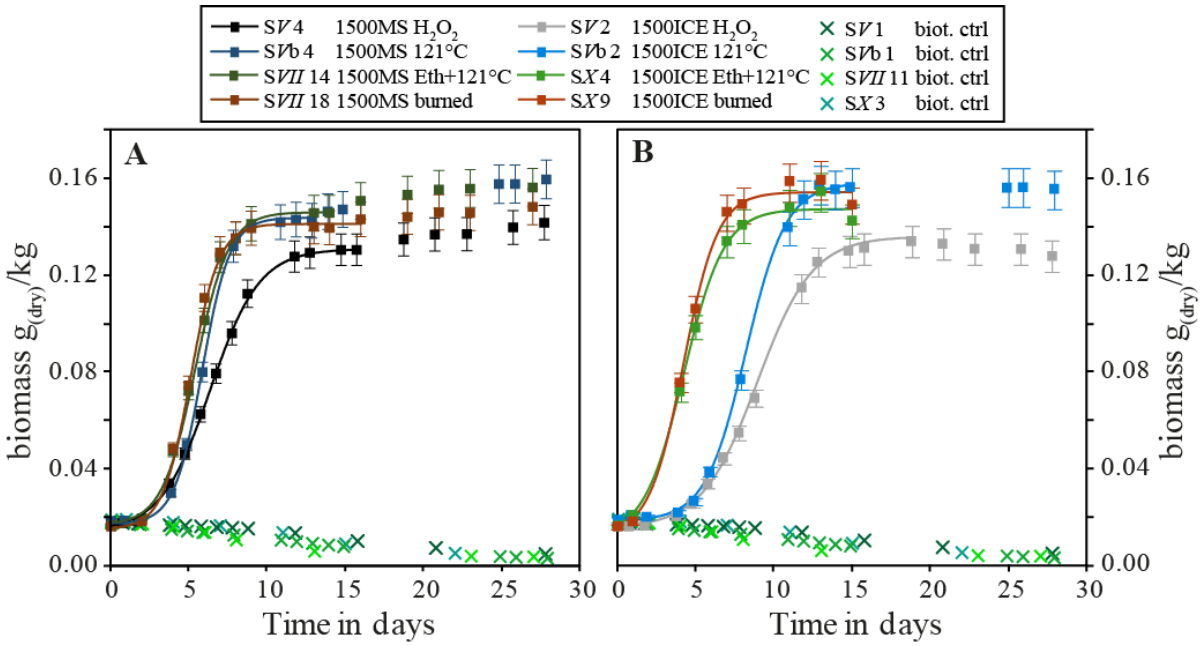

Figure 4. Temporal evolution of biomass concentration during experiments selected to illustrate the effects of the presence of RPM on *Synechococcus sp.* growth in initial fluids having a pH of 5.9. The x-symbols show the results of biotic control experiments performed in the absence of riverine particulate material. Figure A shows experiments performed in the presence of 1500 mg/kg Mississippi RPM and Figure B experiments performed in the presence of 1500 mg/kg Iceland RPM. The different colors indicate the results of experiments run using different protocols for the sterilization of the riverine particulates. The conditions of each experiment are summarized in the legend and provided in Table A1 and A2. The curves indicate the fits of the logistic growth function to each dataset.

The results presented in Figure 4 also illustrate the experimental reproducibility and effect of sterilization protocols. The absence of bacterial growth in the biotic control

experiments performed in the absence of RPM was consistent throughout all the experiments performed at these initial pH conditions. In the presence of 1500 mg/kg Mississippi RPM, the observed growth behavior was very consistent in all plotted experiments with the maximum biomass concentrations varying by only ±5 %. The calculated growth rate constant, μ, and the post-exponential growth behavior, μ_{stat}, among these experiments were reproducible to ±19 and ±26 %, respectively, despite the different sterilization protocols. In the presence of 1500 mg/kg Iceland RPM, the maximum biomass concentration varied by ±8 % and the growth rate constant by 22 % among the plotted experiments. For both types of riverine particulate material, only the reactor where RPM were treated with H_2O_2 showed a slight offset towards lower biomass concentrations.

4.2 The effect of initial biomass concentration on bacterial growth

Figure 5 shows the temporal evolution of biomass concentration of representative growth experiments initiated with different initial biomass concentrations in the presence and absence of 1500 mg/kg MS and ICE riverine particulate material. The experiments were performed at initial pH of 5.9, and containing the 5 % BG-11 media and 3 different initial biomass concentrations 0.007, 0.018, and 0.041 $g_{(dry)}$/kg, represented by different colors in Figure 5. No bacterial growth was observed in the biotic control experiments regardless of the initial biomass concentration; these experiments were performed by placing the initial biomass concentration into reactors with the same initial conditions as the other experiments shown in this figure, but without adding RPM. The bacteria showed typical logistic growth in all experiments performed in the presence of MS and ICE RPM. No significant effect of the different initial biomass concentrations on the bacterial growth was observed as the growth curves were shifted parallel to one another as a function of the initial biomass concentration. However, computed growth rate constants μ increased with decreasing initial biomass concentration (find rates in Table A 2). The post-exponential increase in biomass concentration observed in MS experiments occurred at an average rate of μ_{stat}= $(11.3\pm2.6)\times10^{-04}$ $g_{(dry)}$/kg/day exhibiting a good experimental reproducibility among the different initial biomass concentrations.

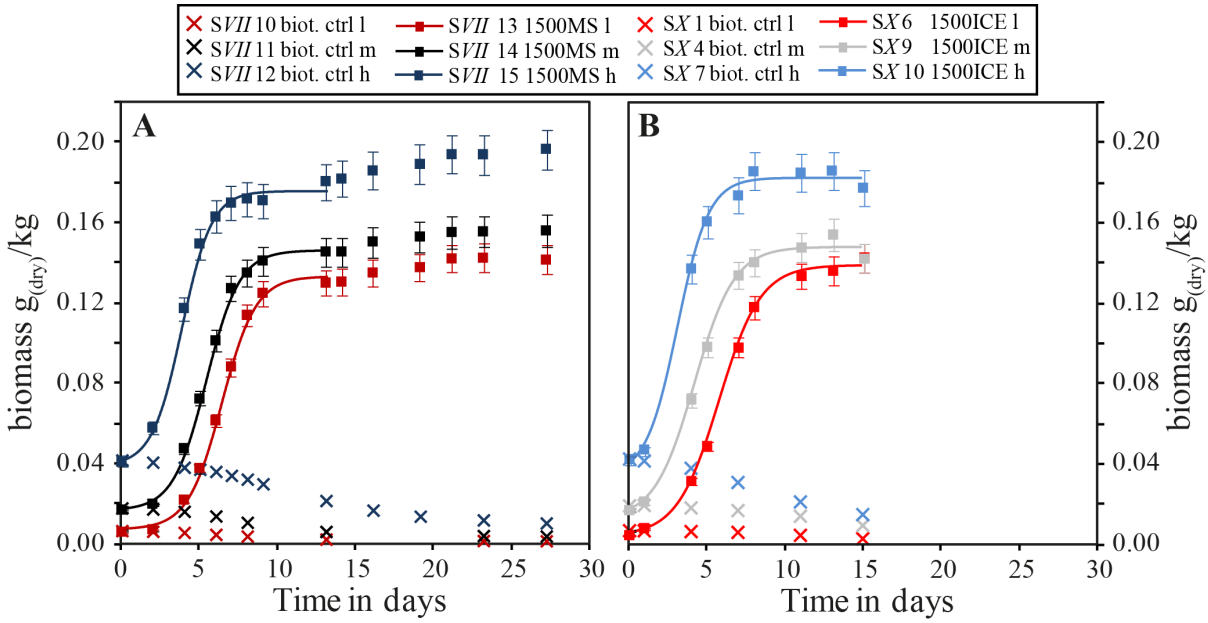

Figure 5. Temporal evolution of biomass concentration in experiments selected to illustrate the effect of initial biomass concentration of growth rates. The x-symbols show results of the biotic control experiments performed in the absence of riverine particulate material. Figure A shows experiments performed in the presence or absence of 1500 mg/kg Mississippi RPM and Figure B experiments performed in the presence or absence of 1500 mg/kg Iceland RPM, which were stopped after the exponential growth phase. The different colors indicate different initial biomass concentrations. The curves indicate the fits of the logistic growth function for each dataset. Details of each experiment are summarized in the legend and presented in Tables A1 and A2.

4.3 Comparison of the effect of Mississippi and Iceland RPM on bacterial growth

Figure 6 shows the temporal evolution of biomass concentration for representative growth experiments organized to illustrate the distinct effects of MS compared to ICE RPM. These experiments were performed in the presence and absence of Mississippi and Iceland RPM at an initial pH of 5.9, in 5 % BG-11 media and a 0.018 $g_{(dry)}$/kg initial biomass concentration. No bacterial growth was observed in the biotic control experiments without additional RPM. Likewise, no bacterial growth was observed in the presence of either 75 mg/kg MS or 75 mg/kg ICE RPM. Notably, the initial biomass concentrations decreased even faster in the presence of 75 mg/kg ICE RPM compared to either 75 mg/kg MS RPM or the biotic control. In the presence of 1500 mg/kg MS and ICE RPM, bacteria showed typical logistic growth, but small differences between MS and ICE experiments were evident. The maximum bacterial growth was observed 2-3 days earlier in the presence of MS RPM compared to ICE RPM (compare Figure 6A and 6B). The post exponential biomass concentration increased in the experiments containing MS RPM; the retrieved μ_{stat} values were $(8.4\pm0.5)\times10^{-04}$ and $(10.6\pm0.5)\times10^{-04}$ $g_{(dry)}$/kg/day for the experiments containing 75 mg/kg MS RPM and 1500 mg/kg MS RPM, respectively. In contrast, the post exponential

biomass concentration tended to decrease in the experiments containing ICE RPM; the retrieved μ_{stat} values were $(-1.7\pm1.6)\times10^{-04}$ and $(-3.7\pm4.3)\times10^{-05}$ $g_{(dry)}$/kg/day for the experiments containing 75 mg/kg MS RPM and 1500 mg/kg ICE RPM, respectively. The measured maximum biomass concentrations were similar for MS (0.142 and 0.159 $g_{(dry)}$/kg) and ICE (0.134 and 0.157 $g_{(dry)}$/kg) RPM. The calculated growth rate constant, μ, was slightly greater in the MS compared to the ICE experiments. Figure 6B also shows the results of two experiments performed in 5 % BG-11 media that were previously equilibrated for one month with 1500 mg/kg MS and ICE RPM and subsequently filtered (0.22 μm filter) to remove the particulates; no particulates were present during the experiments themselves. Again, the exponential growth phase begun notably earlier in the fluid originally equilibrated with MS compared to that originally equilibrated with the ICE RPM. Furthermore, the measured maximum biomass concentration was 19 % higher in the experiment run in the fluid that was originally equilibrated with MS RPM. In both experiments, no post-exponential growth occurred. Note that the total biomass concentrations were much greater in experiments performed in presence of particulates compared to the experiments in which the reactive fluids were previously equilibrated with the RPM and subsequently filtered to remove the particulates (see Figure 6B, filled squares compared to crossed squares).

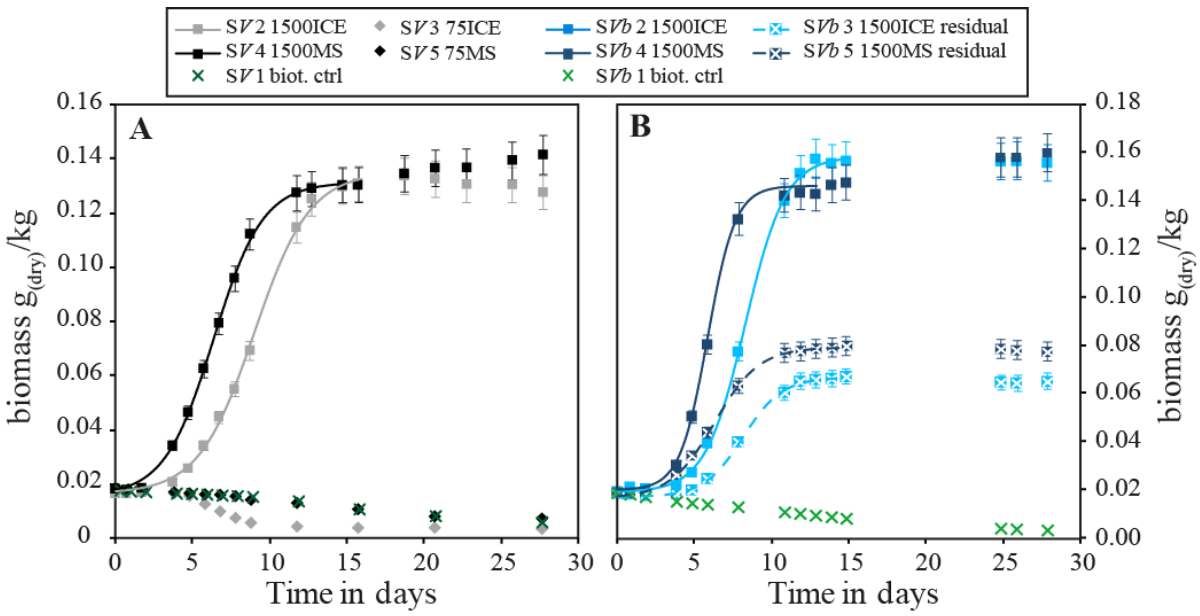

Figure 6. Temporal evolution of biomass concentration during representative experiments run to compare the relative role of MS versus ICE RPM on bacterial growth. The x-symbols show results of biotic control experiments performed without riverine particulate material. Squares indicate results of experiments performed in the presence of 1500 mg/kg Mississippi or 1500 mg/kg Iceland RPM, diamonds represent concentrations of 75 mg/kg of the indicated RPM. The crossed squares in Figure B depict results of experiments performed in fluids originally equilibrated with MS or ICE particulates and subsequently filtered to remove these particles before starting the experiments. The curves indicate the fits of these data to the logistic

growth function to each dataset. Further details of all shown experiments are provided in Tables A1 and A2.

4.4 Effect of different initial conditions on bacterial growth

Figure 7 shows the evolution of biomass, conductivity and pH of seven experiments run at the different initial conditions summarized in Table 3. The results shown in this figure were selected to illustrate the effect of these initial conditions on bacterial growth. Bacterial growth was observed only in the experiment containing 1500 mg/kg MS RPM and in the two experiments run at higher initial pH through the addition of NaOH and $NaHCO_3$ to the initial starting fluid. No growth was observed in the biotic controls run in the absence of RPM, at higher initial conductivity, or in the presence of 1500 mg/kg zircon particles. Note, that maximum biomass concentrations (average of replicates performed at different initial biomass concentrations) were 57±15 % higher in experiments run in the presence of 1500 mg/kg Mississippi RPM compared to the control experiments performed at an elevated initial pH through the addition of NaOH to the initial fluids and 23±9 % higher than the control experiment performed at higher initial pH through the addition of $NaHCO_3$ to the initial fluid (see Figure 7). Furthermore, the biomass concentration in the presence of 1500 mg/kg Mississippi RPM increased steadily after the exponential growth phase, whereas these post exponential growth phase concentrations decreased in the experiments run in the absence of RPM. Details of the pH and conductivity evolution will be discussed in section 0 together with the evolution of the aqueous fluid composition. Figure 8 shows the temporal evolution of biomass concentration of experiments performed in initial fluids where the pH was buffered by the addition of 0.1 mol/kg $NaHCO_3$:Na_2CO_3 in a 90:10 ratio in an initial 5% BG-11 nutrient solution. Instantaneous bacterial growth was observed in all of these experiments, however, the addition of 500 mg/kg MS RPM resulted in 12 and 20 % higher maximum biomass concentrations compared to corresponding control experiments run in the absence of RPM.

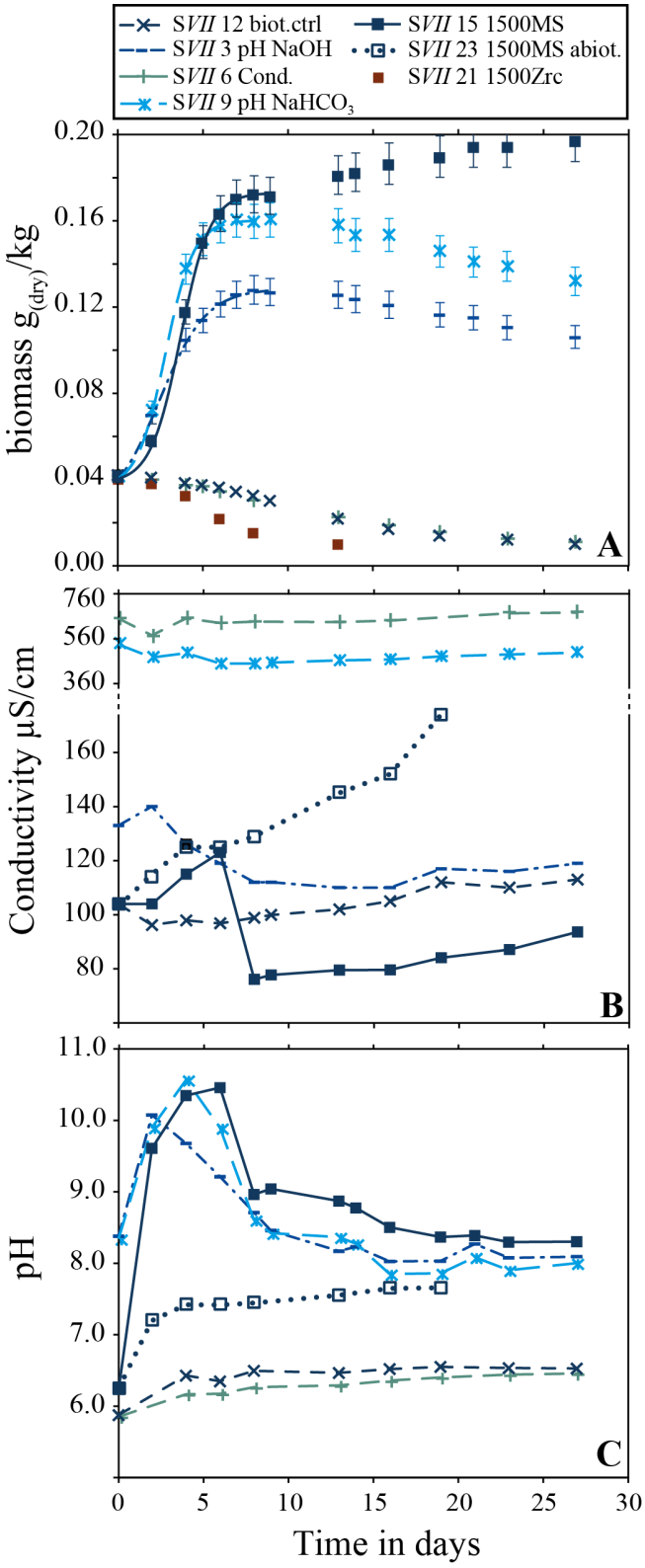

Figure 7. Temporal evolution of biomass concentration (A), conductivity (B) and pH (C) in experiments selected to illustrate the effect of initial fluid compositions on growth. The curves in Figure A show the fits of the logistic growth function, lines in Figures B and C connecting the data points are for the aid of the viewer. Initial conditions for these experiments are summarized in Table 3.

489 **Table 3.** Summary of experimental conditions for the seven experiments performed at
490 different initial conditions to evaluate the potential effect of pH, conductivity, Mississippi
491 (MS) riverine particulate material (RPM) and zircon (Zrc) particles on the growth of
492 cyanobacteria. Corresponding growth plots are shown in Figure 7.

Experiment ID	BG-11 dilution	Initial pH	RPM [mg/kg]	Biomass initial [$g_{(dry)}$/kg]	Conductivity [µS/cm]
S*VII* 12 biot. Ctrl	5%	5.9	--	0.043	104
S*VII* 3 pH NaOH	5%	8.4	--	0.043	133
S*VII* 6 Cond. NaCl	5%	5.9	--	0.043	650
S*VII* 9 pH NaHCO3	5%	8.3	--	0.043	535
S*VII* 15 1500MS	5%	6.2	1500 MS	0.043	104
S*VII* 23 1500MS abiot.	5%	6.3	1500 MS	None	103
S*VII* 21 1500Zrc	5%	n.d.	1500 Zircon	0.041	n.d.

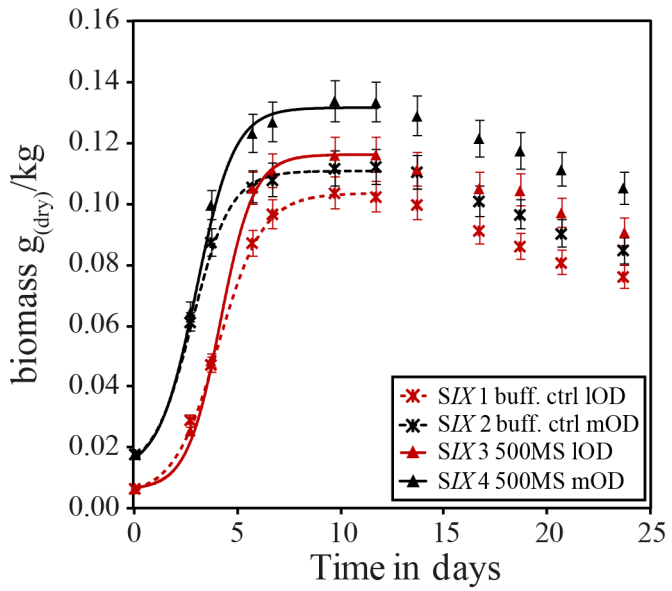

493

494 **Figure 8.** Temporal evolution of biomass concentrations in fluids of experiments performed
495 in carbonate buffer solutions ($pH_{initial}$ = 9.4). The x-symbols illustrate results from biotic
496 control experiments performed in the absence of RPM, triangles illustrate the results of
497 experiments performed in the presence of 500 mg/kg MS RPM. Red symbols illustrate the
498 results of experiments performed at low initial biomass concentrations (0.007 $g_{(dry)}$/kg),whereas
499 black symbols illustrate the results of experiments performed at medium initial biomass
500 concentration (0.018 $g_{(dry)}$/kg). The curves correspond to the fits of each dataset to the logistic
501 growth function to each dataset

502 *4.5 Effect of different riverine particulate material concentrations on bacterial growth*

503 Figure 9 illustrates the effect of different RPM concentrations on bacterial growth.
504 These experiments were performed in 5 % BG-11 media and 0.041 $g_{(dry)}$/kg of initial biomass,
505 and in the absence and presence of various concentrations of MS RPM. Note that
506 corresponding experiments were not performed using the Icelandic RPM. At an initial pH of
507 5.9 (Figure 9A), no bacterial growth was observed in the biotic control in the absence of

508 RPM. The addition of 500, 1000 and 1500 mg/kg MS RPM triggered instantaneous bacterial
509 growth, whereby the maximum biomass concentration increased with increasing RPM
510 concentration. The addition of 75 mg/kg MS particulates provoked growth only after a lag
511 phase of about twenty days. Furthermore, the post-exponential increase in biomass
512 concentration was more pronounced at higher RPM concentrations. At the higher initial pH of
513 6.8 (Figure 9B), bacteria in all experiments, including the biotic control experiment run in the
514 absence of RPM grew instantaneously. The effect of higher initial pH on the growth of the
515 biotic control experiment was also observed in the other experiments described above.
516 However, with increasing RPM concentration, exponential growth was observed earlier and
517 the maximum biomass concentrations were higher. The measured maximum biomass
518 concentrations presented in Figure 9B increased by 5, 16, 19 and 32 % with the addition of
519 75, 500, 1000 and 1500 mg/kg MS RPM compared to the biotic control experiment. Again,
520 the post-exponential increase in biomass concentration was more pronounced in the presence
521 of higher RPM concentrations. Figure 10 illustrates the effect of different RPM concentrations
522 on bacterial growth in experiments performed at 2.67 times higher initial nutrient
523 concentrations (13.3% BG-11 media). The biotic control experiment performed in the absence
524 of RPM showed bacterial growth only after a lag phase of about two weeks, whereas
525 experiments run in the presence of Mississippi RPM showed either instantaneous bacterial
526 growth or a significantly shorter lag phase. Furthermore, the there is clearly a trend of an
527 increased maximum biomass concentration with increasing RPM concentration. The
528 measured maximum biomass concentrations presented in Figure 10 increased by 6, 14, 15 and
529 21 % with the addition of 75, 500, 1000 and 1500 mg/kg MS RPM compared to the biotic
530 control experiment. The post-exponential bacteria growth is also clearly a function of the
531 mass of MS RPM added to the reactors; the post-exponential growth rate is negative in the
532 presence of 0 or 75 mg/kg MS RPM but positive at higher MS RPM concentrations.

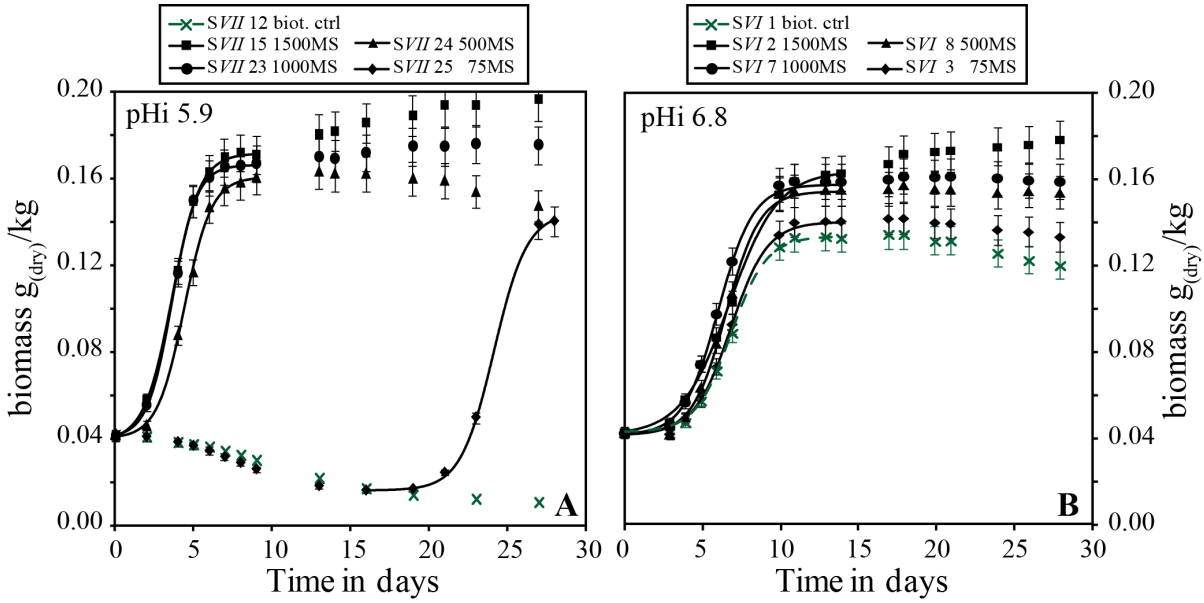

Figure 9. Temporal evolution of biomass concentration in experiments selected to illustrate the effect of RPM concentration on bacteria growth rates: (A) experiments performed at an initial pH of 5.9 and (B) experiments performed at an initial pH of 6.8. The x-symbols indicate the results of biotic control experiments performed in the absence of, RPM, whereas the filled diamonds, triangles, circles and squares represent results of experiments performed in the presence of 75, 500, 1000 and 1500 mg/kg Mississippi RPM, respectively. The curves indicate the fits of the logistic growth function to each dataset and the identity of each experiment is provided in the legend.

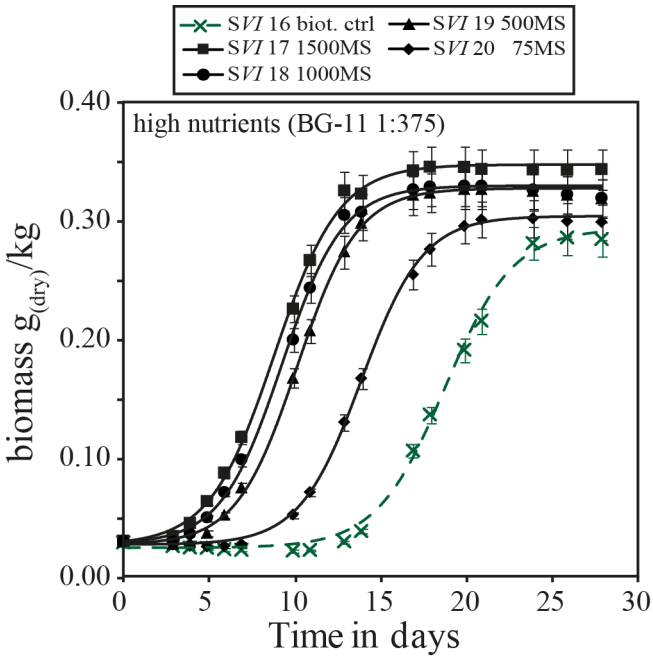

Figure 10. The evolution of biomass concentration in experiments selected to illustrate the effect of RPM on bacteria growth rates at elevated initial nutrient concentrations. The x-symbols represent the results of biotic control experiments performed in the absence of particulate material, whereas the filled diamonds, triangles, circles and squares represent the results of experiments performed in the presence of 75, 500, 1000 and 1500 mg/kg Mississippi RPM, respectively. The curves indicate the fits of the logistic growth function to each dataset, and the legend provides the identity of each experiment.

4.6 The temporal evolution of the reactive fluid compositions

4.6.1 The temporal evolution of pH and dissolved inorganic carbon (DIC)

Figure 11 shows the temporal evolution of biomass, pH and DIC concentration of the reactive fluids collected during selected experiments. In the biotic control experiment run in the absence of RPM, no growth was observed and pH increased slightly from initially 5.9 to a final pH of 6.6. In the abiotic control experiments run in the presence of RPM but the absence of added *Synechococcus sp*., the pH increased from 5.9 to 7.6 and to 7.0 for reactors containing 1500 mg/kg MS and ICE RPM, respectively. In the biotic experiments containing 1500 mg/kg MS and ICE RPM, the bacterial growth resulted in a pH increase from an initial pH of 5.9 to 10.6 and 10.1, respectively. The elevated pH persisted during the exponential growth phase and was followed by a pH drop to final values of 8.2 and 7.6, respectively. This pH evolution is closely linked to the Dissolved Inorganic Carbon (DIC) concentration. In the biotic control experiment run in the absence of RPM, DIC concentrations were constant at 0.7 - 0.9 ppm throughout the experiment. In the abiotic control experiments containing 1500 mg/kg MS RPM but in the absence of added *Synechococcus sp*., the DIC increased from 0.8 to 4.9 ppm during the experiment, while DIC in the abiotic control experiment containing 1500 mg/kg ICE RPM only slightly increased from 0.8 to 1.4 ppm. The greater increase observed in the presence of MS compared to ICE RPM is consistent with the higher pH in MS experiments and the increasing solubility of $CO_{2(g)}$ at higher pH. In both biotic experiments performed in the presence of RPM, DIC increased significantly as a consequence of increasing pH stemming from the photosynthetic activity of the growing bacteria. During the exponential growth phase, DIC increased from 1.0 to 8.5 ppm and from 0.8 to 6.6 ppm in the presence of 1500 mg/kg MS and of 1500 mg/kg ICE RPM, respectively. After the exponential growth phase was complete, DIC increased slightly from 8.5 to 9.6 ppm in the MS experiment but decreased from 6.6 to 5.3 ppm in the ICE experiment.

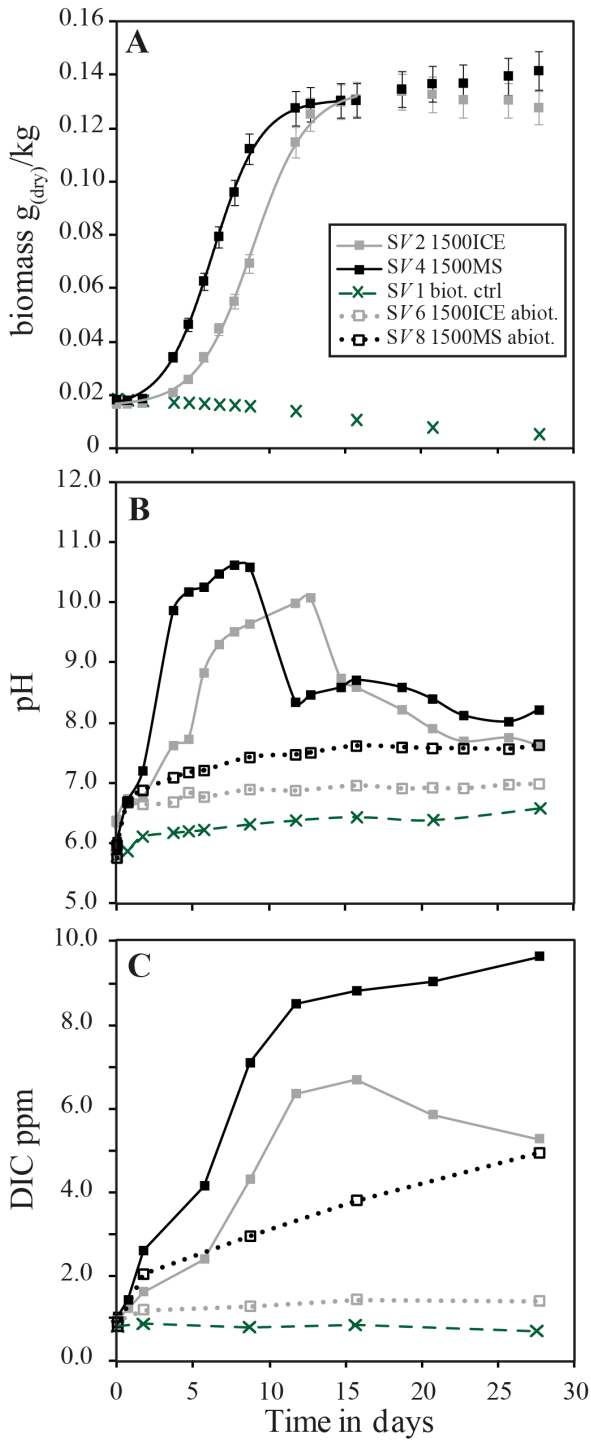

Figure 11. Temporal evolution of biomass concentration (A), pH (B) and dissolved inorganic carbon (C) in selected experiments. Crosses represent the results of biotic control experiments performed in the absence of RPM, filled squares indicated experiments performed in the presence of either 1500 mg/kg MS or 1500 mg/kg ICE. Open squares illustrate results of abiotic control experiments performed in the in the presence of either 1500 mg/kg MS or 1500 mg/kg ICE, but in the absence of added *Synechococcus sp*. The curves in Figure A show the fits of the data to the logistic growth function; lines in Figures B and C connecting the data points are for the aid of the viewer. The identity of each experiment is provided in the legend.

4.6.2 The evolution of major and trace elements

Figure 12 shows the temporal evolution of various elements in fluid samples collected from selected experiments. The green dashed line represents the results of the biotic control experiment performed in the absence of RPM, the open squares depict the results of abiotic control experiments run in the presence of 1500 mg/kg MS or 1500 mg/kg ICE RPM but in the absence of added *Synechococcus sp*., and the filled squares depict the results of experiments run with both added RPM and bacteria. Note that no growth was observed in the biotic control experiments run in the absence of RPM (see Figure 11A). Figure 12A depicts the temporal evolution of Si concentration; Si concentration increases in the fluids due to the dissolution of silicate minerals. The dissolved Si concentration in the biotic control experiment run in the absence of RPM remained constant at 218±36 ppb.

Dissolved silicon concentrations in the abiotic and biotic reactors containing Mississippi RPM showed an initial increase from 225 ppb and 116 ppb to 367±34 ppb and 382±25 ppb, where they remained constant throughout the rest of the experiments. Dissolved silicon concentrations in the abiotic experiments and the biotic experiment containing Iceland RPM increased during the first five days from 206 ppb and 144 ppb to 994±12 ppb and 1064±18 ppb. During the following 22 days, the dissolved Si concentration of the fluid during the biotic experiment run in the presence of ICE RPM increased to a much greater extent reaching a final concentration of 4360±8 ppb compared to 2221±8 ppb for the corresponding abiotic control experiment. A similar temporal evolution was observed for dissolved aluminum concentrations.

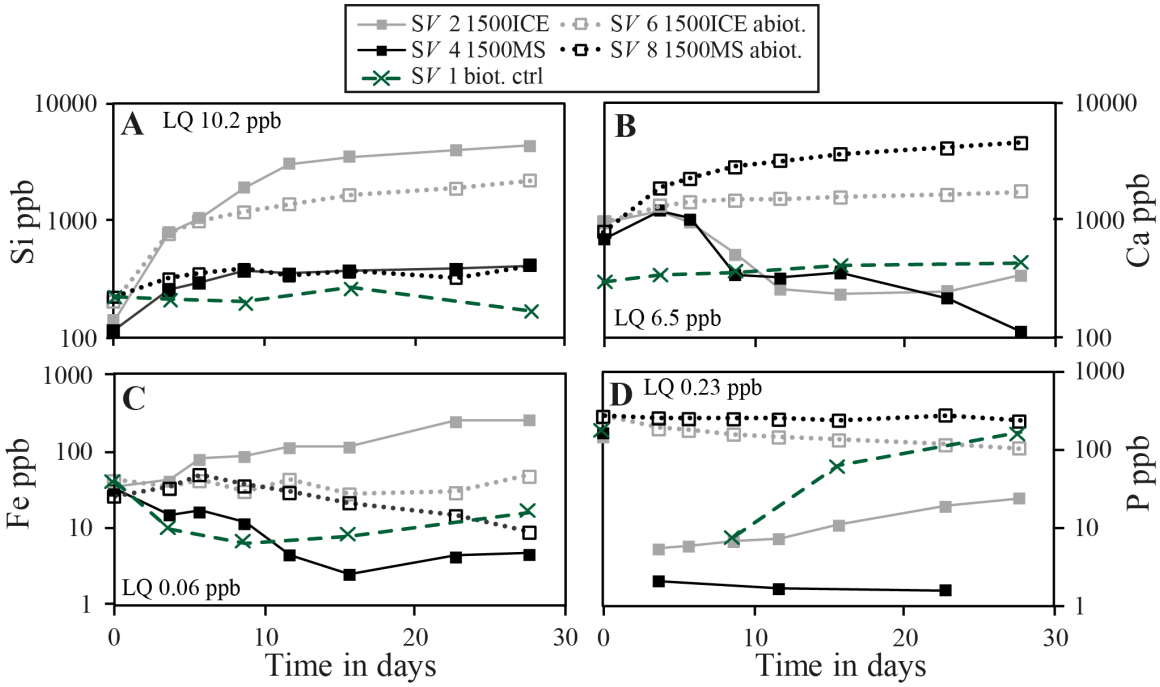

Figure 12. Temporal silicon (A), calcium (B), iron (C) and phosphorus (D) concentration of the fluid phases of selected experiments obtained by ICP-MS analyses. The x-symbols correspond to concentrations of biotic control experiments, run in the absence of particulate material; filled squares correspond to results experiments performed in the presence of either 1500 mg/kg MS or 1500 mg/kg ICE RPM. Open squares represent the results of abiotic control experiments performed in the presence of either 1500 mg/kg MS or 1500 mg/kg but the absence of added *Synechococcus sp*. The lines connecting data points are for the aid of the viewer. The identity of each experiment is provided in the legend, and further details of each experiment in Tables A1 and A2.

Figure 12B shows the temporal evolution of dissolved Ca concentration during selected experiments. The calcium concentration in the biotic control experiment performed in the absence of added RPM increased from 294±2 ppb to 432±3 ppb during this experiment. The dissolved Ca concentration in the abiotic control experiment increased from its initial 803±5 ppb and 970±3 ppb to 4567±16 ppb and 1776±8 ppb in the presence of Mississippi and Iceland RPM, respectively. In the biotic experiments containing either MS or ICE RPM, Ca concentrations increased during the first four days from 694±9 ppb and 956±5 ppb to 1221±2 ppb and 1221±1 ppb, then decreased to 113±1 ppb and 234±7 ppb, respectively. Similar trends were observed for the concentrations of Mn and Mg.

Figure 12C and 12D show the temporal evolution of dissolved Fe and P concentrations, representing possible limiting nutrients. Initial dissolved Fe concentrations were at 35±6 ppb in all reactors. In the biotic control experiments run in the absence of RPM, Fe concentration decreased during the first days to 6 ppb and subsequently increased to a final concentration of

16 ppb at the end of the experiment. In the abiotic control experiment run in the presence of 1500 mg/kg MS RPM, but in the absence of added *Synechococcus sp*., the dissolved Fe concentration decreased to 9 ppb, whereas the dissolved Fe concentration remained constant at 37±8 ppb in the abiotic control experiment containing 1500 mg/kg ICE RPM. Similarly, the biotic experiments containing either 1500 mg/kg MS or 1500 mg/kg ICE RPM showed distinct temporal dissolved Fe concentration evolutions. In the biotic MS experiment, dissolved Fe decreased to about 4 ppb, whereas Fe concentrations in the biotic ICE experiment increased continuously to 257±4 ppb. Dissolved phosphate concentrations were initially at about 260 ppb in all reactors. In the biotic control experiment in the absence of RPM, the dissolved P concentration initially dropped below detection limit and subsequently increased again towards its initial concentration. Dissolved P concentration remained constant in the abiotic control experiment run in the presence of 1500 mg/kg MS RPM at 251±15 ppb, whereas it decreased steadily in the corresponding abiotic experiment run in the presence of ICE RMP from initially 262±2 ppb to 105 ppb. In the biotic MS and ICE experiments, dissolved P concentrations initially dropped to less than 10 ppb. In the biotic MS experiment, the concentration remained near zero throughout the experiment. In the biotic ICE experiment, the initial drop in P concentrations was followed by a steady increase to a final concentration of 24 ppb.

4.7 SEM investigation of riverine particulate material

A few mg of the ICE and MS riverine particulate material sampled from the exponential growth phase of the bacteria during selected experiments were investigated by SEM. Figure 13A-D show representative SEM images of sampled Mississippi particulate material. No morphological differences were evident between the initial particulates and the particulates sampled during bacterial growth, but occasionally, bacteria were found attached to feldspar grains (Figure 13B). Clusters of agglomerated bacteria were frequent, as evident in Figure 13A and depicted in detail in Figure 13C. These agglomerates were associated with mineral

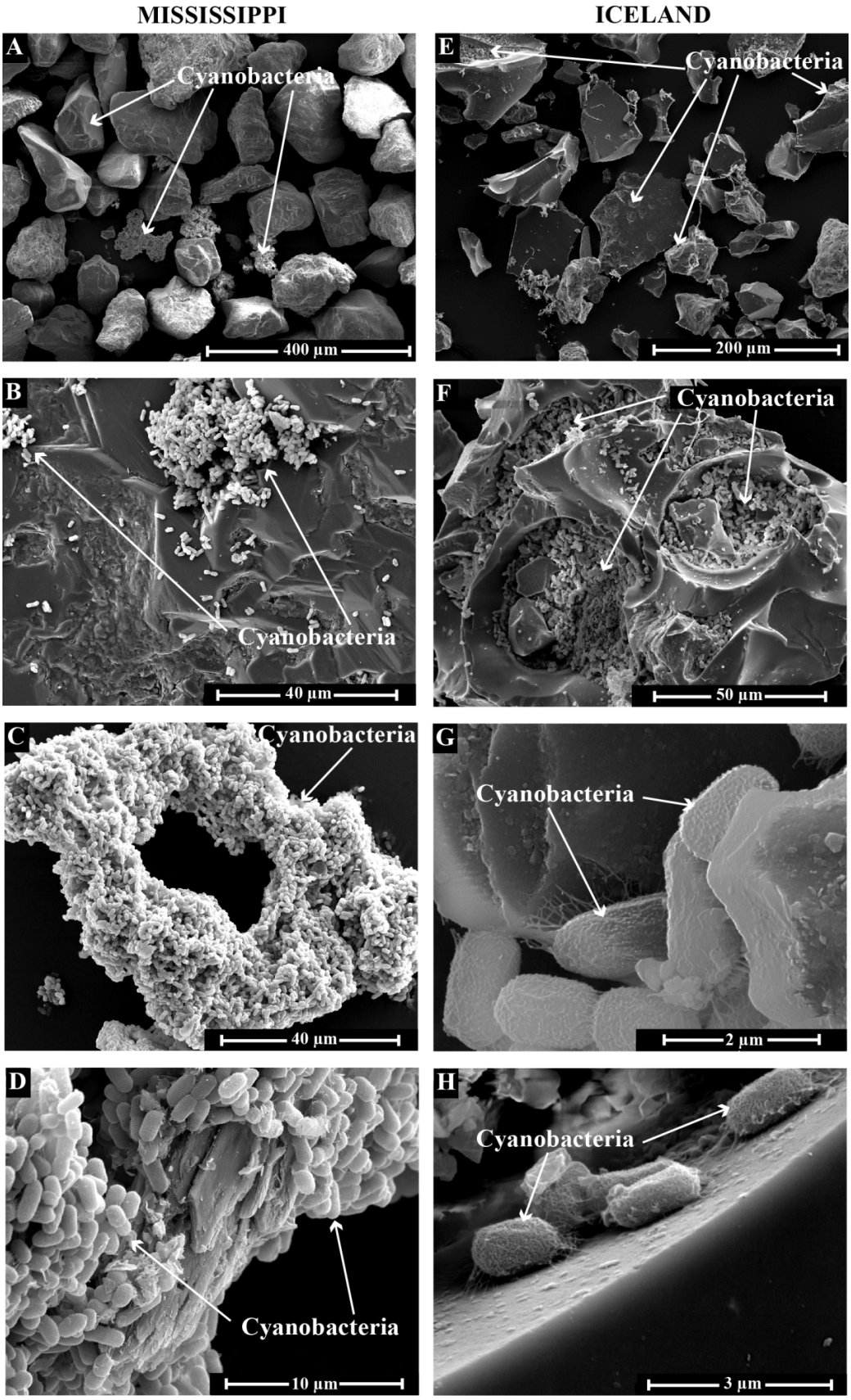

Figure 13. SEM microphotographs of Mississippi (A-D) and Iceland (E-H) riverine particulate material sampled during the exponential growth phase collected during experiments S*III* 5 15000MS and S*III* 3 1500ICE, respectively (see Table A1).

fragments (Figure 13D), predominantly clays. Figures 13E-F show representative images of sampled Iceland particulate material. Again, no major morphological changes are evident compared to the initial material. The basaltic glass particles were, however, frequently covered by cyanobacteria, as indicated in Figure 13E and illustrated in Figure 13F. The bacteria appeared mostly in vesicles of basaltic glass particles. In closer detail, the cyanobacteria were found to be attached to the glass surfaces via organic fibers (Figure 13G and Figure 13H). Note, that the bacteria attached on these surfaces are not accounted for in the spectrophotometric determination of biomass concentration due to settling of particles in the cuvette. Consequently, the total biomass concentration in experiments containing RPM is potentially higher than the values reported.

5. Discussion

5.1 The effects of riverine particulate material on the growth of Synechococcus sp. freshwater cyanobacteria

The results presented above illustrate the effects of riverine particulate material on the growth of *Synechococcus sp.* freshwater cyanobacteria. Firstly, at low initial nutrient concentrations and an initial pH of 5.9, the presence of Mississippi and Iceland RPM triggered bacterial growth, whereas bacteria cultures in biotic controls without riverine particulates did not grow. This growth triggering effect is best illustrated in Figures 4, 5, 6, 7A, 9A and 11A. In growth experiments performed at higher initial pH, bacterial growth was observed in the biotic control experiments, as illustrated in Figures 7A, 8, and 9B. Similarly bacterial growth was observed in biotic control experiments in an experiment run at high initial nutrient concentrations (see Figure 10). Bacterial exponential growth, however, occurred earlier in the presence of riverine particulate material. This is best illustrated in Figure 10, where the maximum bacterial growth was observed after 8.7, 9.1, 10.0 and 13.8 days in growth experiments performed in the presence of 1500, 1000, 500 and 75 mg/kg MS RPM, but only after 18.7 in the biotic control experiment without RPM. Furthermore, the maximum biomass concentrations increased as a function of RPM concentration. This effect is summarized for all experiments containing Mississippi RPM in Figure 14, which shows the highest biomass concentration measured in each experiment plotted against the MS RPM concentration added to the reactors. The illustrated biotic control experiments run in the absence of RPM were all conducted at $pH_{inital} \geq 6.8$ as no growth was observed at lower pH. The biomass concentration in these biotic RPM free experiments is limited by the initial nutrient concentration and varies as a function of the initial BG-11 concentration used in each

experiment (the black symbols in this figure show experiments performed at higher nutrient concentration). Additional bacterial growth at a given initial BG-11 concentration only occurs from the additional nutrients delivered from dissolving the riverine particulates. To a first approximation, the maximum biomass concentration increased linearly with increasing MS RPM concentration as shown in Figure 14 by the linear regression of the data. The maximum biomass concentration increased by $(2.5\pm0.5)\times10^{-5}$ at low initial nutrient concentrations and $(4.8\pm0.9)\times10^{-5}$ $g_{(dry)}$/kg at high initial nutrient concentrations with each mg/kg MS RPM added to the reactor. For the low initial nutrient experiments run here, this yields an average increase of about 15, 35 and 32 % for the addition of 500, 1000 and 1500 mg/kg MS riverine particulate material compared to biotic control experiments run in the absence of RPM. The presence of riverine particulates also influenced the evolution of the biomass concentration during the stationary phase. The presence of MS RPM resulted in a continuous increase of the biomass concentration after the exponential growth phase, whereas biomass concentration stayed constant or decreased when no particulates were added to the reactors. This observation is most evident in Figure 7A, where bacteria concentration continuously increased during the stationary growth phase in the presence of 1500 mg/kg MS RPM but notably decreased in biotic control experiments run in the absence of particulates. Figure 9 illustrates the same effect as a function of particulate concentration. Figure 15 summarizes the post-exponential growth behavior obtained by linear regression of the biomass concentrations as a function of the MS RPM concentration measured after the exponential growth phase was completed. In the biotic control experiments, the stationary phase biomass concentrations decreased at an average rate of μ_{stat}= $(-12.0\pm6.2)\times10^{-4}$ $g_{(dry)}$/kg/day. With increasing MS RPM concentration this rate became positive, reaching μ_{stat}= $(+9.3\pm3.6)\times10^{-4}$ $g_{(dry)}$/kg/day in the presence of 1500 mg/kg MS particulates.

In summary, riverine particulate material has three major effects on the growth of freshwater cyanobacteria *Synechococcus sp*. First, RPM triggers bacterial growth if the pH of the aqueous fluid is below 6 by increasing fluid pH. Second, the presence of RPM increases the total maximum biomass concentration during the experiments and third, the presence of particulate material causes a post-exponential long-term growth of the cyanobacteria. In all cases these effects become more pronounced with increasing RPM concentration. However, the presence of RPM is expected to lower light availability which might limit bacterial growth. Under the applied experimental conditions, it is unlikely that light limits growth since biotic control experiments in the absence of light blocking particulate material would have shown higher biomass concentrations due to higher availability of light.

5.2 How does riverine particulate material increase bacterial growth?

To evaluate the factors triggering bacterial growth in the presence of RPM, five possible influencing factors were tested: 1) the addition of organic compounds contributed to the fluid by the particulates, 2) the physical presence of particulate surfaces, 3) the slight increase in ionic strength resulting from dissolving particulates, 4) a pH increase resulting from particulate dissolution, and 5) an increased nutrient concentration due to particulate dissolution. To address these factors, growth experiments were performed with distinct initial conditions including: 1) RPM burning at 450 °C to remove potential organic compounds, 2) addition of zircon particles to provide the presence of inert mineral surfaces, 3) higher initial ionic strength of the fluids by the addition of NaCl, 4) higher initial pH by addition of NaOH or carbonate buffers and 5) higher initial nutrient concentrations.

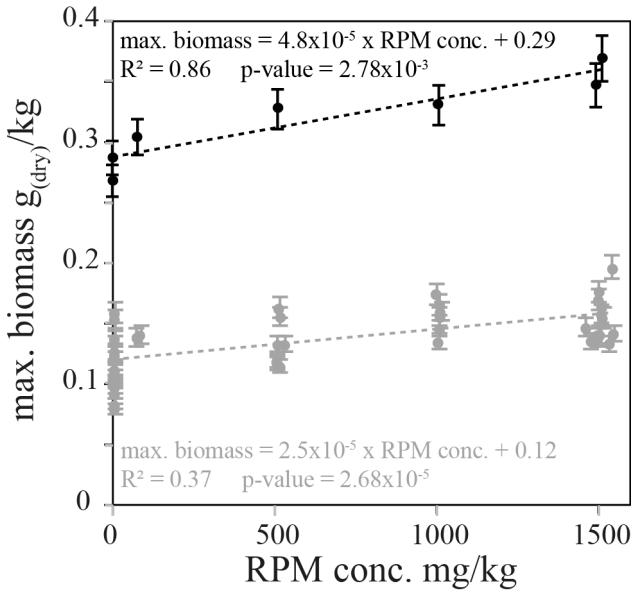

Figure 14. Highest biomass concentration measured in all experiments where growth was observed as a function of the mass of Mississippi RPM added to the reactors at the beginning of each experiment. The results of biotic controls containing zero RPM shown in this figure were all run at an initial pH≥6.8. The black symbols indicate experiments performed in fluids having an elevated initial nutrient concentration (13.3 % BG-11 media), the grey symbols indicate experiments performed at lower initial nutrient concentrations (5 % BG-11 media). The dotted lines represent linear regressions of the data.

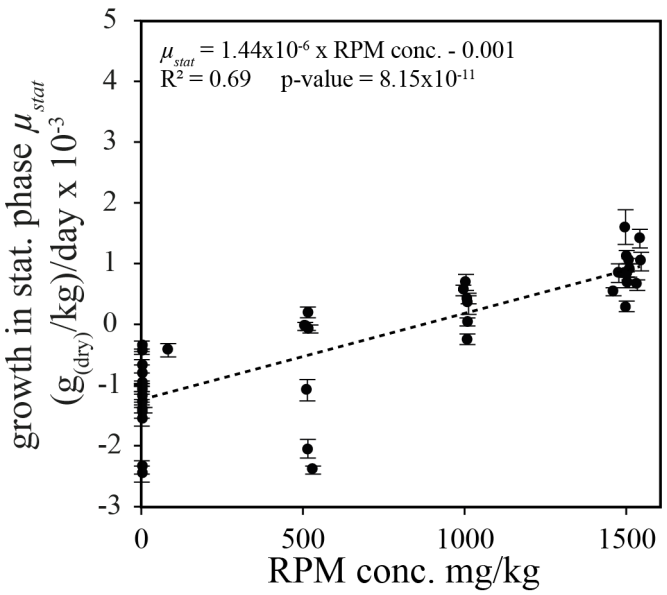

Figure 15. *Synechococcus sp* stationary phase growth rates as a function of Mississippi RPM concentration. The biotic controls run in experiments containing zero RPM shown in the figure were run in fluids having an initial pH≥6.8. The illustrated stationary phase growth rates, μ_{stat} were obtained by the linear regression of the biomass concentrations measured in experiments after the completion of the exponential growth phase. The dotted line depicts a linear regression of the measured rates.

Results of these experiments are shown in Figures 4, 7, 8 and 10. Figure 4 shows the evolution of biomass of four experiments performed with different protocols applied for the sterilization of the riverine particulate material. To eliminate a potential organic contamination introduced to the fluid by the RPM, the particulates were sterilized by either a H_2O_2 treatment, by dry sterilization at 121 °C for 12 h with or without previous ethanol treatment, or by heating for 2.5 h at 450 °C. Similar bacterial growth was observed in all reactors suggesting that organic contamination from the particulates was not a major factor influencing growth rates and that different treatments did not result in major surface change effects. Only the experiments where the RPM were treated with H_2O_2 showed a slight offset towards lower biomass concentrations.

Figure 7 shows the evolution of biomass, conductivity and pH of seven reactors run at the distinct initial conditions summarized in

764 Table **3**. In the biotic control experiments performed at higher initial pH, bacteria
765 showed logistic growth, however, to 23-57 % lower final biomass concentrations compared to
766 experiments run in the presence of 1500 mg/kg Mississippi RPM. This observation suggests
767 that the initial growth triggering effect of the RPM stems at least in part from the increase in
768 pH caused by the dissolution of the particulates. This is in agreement with growth
769 experiments performed by Bundeleva et al. (2014) who observed that this species only grows
770 at pH ≥7.3. Neither the presence of zircon nor increasing ionic strength altered bacterial
771 growth rates. However, the biotic control where pH was increased by the addition of $NaHCO_3$
772 to the initial fluid phase showed higher maximum biomass concentrations compared to the
773 control where initial pH was increased by the addition of NaOH. This suggests that the
774 availability of dissolved carbonate also enhances bacterial growth. Thus, a series of
775 experiments was performed in carbonate buffer solutions (0.1 mol/kg DIC) designed to keep
776 pH constant but provide various quantities of C for bacterial growth. These results, presented
777 in Figure 8, show that even at these conditions, the presence of 500 mg/kg Mississippi RPM
778 increased the maximum biomass concentrations by 12 and 20 % compared to corresponding
779 control experiments run in the absence of RPM. Similarly, the presence of RPM resulted in 6-
780 21 % greater biomass concentrations in experiments containing high initial nutrient
781 concentrations (see Figure 10).

782 In summary, results indicate that one factor leading to increased biomass in the presence
783 of RPM is the increase of pH due to mineral dissolution. Nevertheless, even at favorable
784 initial conditions (higher initial pH, carbonate buffered fluid or higher initial nutrient
785 concentration), the presence of RPM resulted in 1) higher maximum biomass concentrations
786 and 2) a continuous post-exponential increase in biomass concentration. The post-exponential
787 growth was only evident for MS particulates, which were studied in more detail. These three
788 positive effects of RPM on bacterial growth might result from the creation of
789 microenvironments around the cells favorable for CO_2 uptake necessary for cyanobacteria
790 growth through the adjustment of pH and the release of nutrients. To illuminate the hypothesis
791 of nutrient release from the RPM as trigger for additional growth, the chemical evolution of
792 the fluid phase was investigated in selected experiments and results are presented in Figures
793 11 and 12. Note, that the interpretation of the fluid composition in these experiments is
794 challenging since multiple biogeochemical processes occur simultaneously. Besides the
795 dissolution of the riverine particulate material and the consumption of nutrients by growing
796 cyanobacteria, processes as secondary phase precipitation and/or the ad- and desorption of
797 elements on mineral or bacteria surfaces may influence the temporal evolution of each

element. Furthermore, changes in pH and dissolved organic matter concentration can change the solubility and/or speciation of elements in the fluid phase during our experiments. Figure 12A shows the evolution of Si concentration, which changes due to silicate mineral or glass dissolution. Two important observations are evident in this figure. First, the silicates in Iceland RPM dissolve faster than those in Mississippi particulates. Note that Mississippi RPM is primarily composed of quartz and feldspar, whereas Iceland RPM is composed of basalt and basaltic glass which dissolve faster at these conditions (Gislason and Oelkers, 2003). Second, the silicate minerals and glass in the biotic reactors dissolve faster compared to those in the corresponding abiotic experiments, in part due to the pH increase induced by growing cyanobacteria and the decreased stability of alumosilicate minerals at higher pH. Figure 12B shows the temporal evolution of Ca concentration. Again, two important observations are evident in this figure. First, Mississippi RPM releases far more Ca (as well as Mn and Mg) to the fluid compared to Iceland RPM, likely due to presence of trace amounts of carbonate minerals in these RPM. Second, in the biotic experiments run in the presence of MS and ICE RPM, Ca concentrations dropped after a few days. This drop in Ca (also observed for Mg and Mn) coincides with the drop in conductivity (see Figure 7B) and may stem from the precipitation of carbonate minerals triggered by increasing pH due to the metabolic activity of the growing cyanobacteria. Figure 12C and 12D show the temporal evolution of Fe and P concentrations. The ICE particulates delivered much more Fe to the fluid compared to the MS RPM, which did not, however, result in a more pronounced bacterial growth as can be seen in Figure 11A. Dissolved phosphate concentrations in all biotic experiments indicate complete consumption of this element by the biomass, even in the biotic control experiments in run in the absence of RPM, where no growth was observed. The close to zero dissolved P concentrations throughout the biotic experiment containing 1500 mg/kg MS RPM (experiment S*V* 4 1500MS), which exhibited post-exponential bacterial growth, suggests that this growth was P limited. However, MS RPM did not release significant amounts of P to the fluid phase in the absence of bacteria as indicated by the results of the corresponding abiotic control experiment. It is noteworthy that MS RPM showed a greater increase in biomass compared to the ICE RPM, even though Iceland particulates contain much more Fe and P and the silicate minerals and glass in these particulates dissolve more rapidly. One possibility is that the attachment of bacteria to the surface of the minerals in this RPM limits particle dissolution of mafic minerals such as observed by Oelkers et al. (2015). We suggest that certain accessory phases, such as carbonates or clay minerals, which readily exchange their interlayer cations, or the presence of highly reactive nanoparticles adhering to larger grains

(Poulton and Raiswell, 2005) potentially present in the MS RPM might be most efficient in increasing bacterial growth. Furthermore, the stronger effect of Mississippi particulates might stem from a higher concentration of adsorbed nutrients on MS particle surfaces as these particles would have been impacted by anthropogenic and agricultural activity.

The SEM investigations of the riverine particulate material showed that cyanobacteria were frequently found attached through organic fibers on particle surfaces, especially on clays in Mississippi RPM and on basaltic glass fragments in Iceland RPM (see Figure 13). This direct attachment of microbes on the particle surfaces suggests that the cyanobacteria are able to directly acquire the limiting nutrient from the minerals through an increase in production of exopolymeric substances (EPS) and transparent exopolymeric particles (TEP). The ability of microbes to acquire limiting nutrients directly from the mineral phase has been shown by numerous past studies including Bailey et al. (2009), Rogers et al. (1998), Rogers and Bennett (2004), Bonneville et al. (2011), Smits et al. (2012) and Sudek et al. (2017). Note, that these observation were all made for heterotrophic or benthic microorganisms and not photoautotrophic, planktonic bacteria as in our study.

The direct attachment of bacteria on the mineral surface together with the alkaline pH produced by the bacteria can increase the dissolution rate of the silicate minerals and glasses present in the particulates. This has been shown in numerous studies (Bennett et al., 2001; Drever and Stillings, 1997; Olsson-Francis et al., 2012; Rogers and Bennett, 2004; Uroz et al., 2009; Wu et al., 2007; 2008). In this study, bacteria likewise indirectly enhanced mineral dissolution by altering pH and potentially also through the production of organic ligands. This creates a positive interplay between bacteria and minerals where mineral dissolution enhances bacterial growth though nutrient release and the enhanced bacterial activity accelerates mineral dissolution through altering the aqueous solution concentration. This feedback may also be facilitated and enhanced by the direct attachment of the bacteria to the mineral surfaces.

5.3 Potential role of riverine particulate material in natural environments

The potential role of river transported particulate material on global element cycles has received attention as particulates dominate the transport of limiting nutrients compared to dissolved riverine transport (Jeandel and Oelkers, 2015). Nutrients transported in particulate form likely act as slow release fertilizer promoting bacterial growth. The results obtained in

this study validate the role of particulate material on productivity in freshwater environments and suggest that such particles influence the natural biotic carbon cycle.

The results presented in this study suggest that riverine particulate material can enhance bacterial growth in natural nutrient limited systems. Moreover, in certain environments, particulates might trigger calcite precipitation. A number of studies described calcite precipitation induced by algae or cyanobacteria blooms in natural lakes (Hodell et al., 1998; Stabel, 1986; Thompson et al., 1997). Notably, Thompson et al. (1997) emphasized that *Synechococcus sp.* cyanobacteria are especially suitable for calcite precipitation and observed calcite precipitates in the alkaline microenvironment around the cells. Thompson et al. (1997) furthermore mentioned that *Synechococcus sp.* exhibit a benthic growth habit, colonizing various surfaces. As shown in this study, dissolving particulates can provide limiting nutrients for bacterial growth and may act as substrates on which bacteria can grow. The physical contact between the cells and the particle surface can accelerate their dissolution, thus liberating, depending on the mineralogy of the particulates, divalent cations ready to form carbonates. Thus, we hypothesize a potential role of particulate material in triggering algae blooms and simultaneously occurring whiting events.

Phytoplankton blooms commonly occur during spring and early summer, when temperature rises and light availability is maximize. During spring, however, fluxes of riverine particulate material also maximize. Gislason et al. (2006) reported a variation in Ca particulate fluxes of 4.5 orders of magnitude over the course of a year in a glacial river in NE Iceland with maximum particulate fluxes during spring and late summer. Thus, times of increased primary production coincide with times of highest particulate nutrient fluxes. The effect of riverine particulate material on phytoplankton growth in natural systems, however, requires a case-by-case study depending on various environmental factors such as nutrient availability and nutrient ratios, light conditions and the distribution of phytoplankton species. For example, Baisre and Arboleya (2006) described a drastic reduction in nutrient concentrations resulting from decreasing sediment concentration in a Cuban estuary following upstream dam constructions. This had a profound negative influence on the estuary ecosystem and hence, on local fisheries. In contrast, Jiang et al. (2014) and Chen et al. (2017) observed increasing chlorophyll *a* concentrations with decreasing suspended sediment input in Chinese estuaries, as a consequence of dam constructions. This might occur in highly eutrophic systems, where light availability limits primary productivity.

The global impact of river damming on biogeochemical cycles has long been recognized and numerous studies described the degree and the consequences of retention of particulates and nutrients in dammed river systems (Baisre and Arboleya, 2006; Bergkamp et al., 2000; Eiriksdottir et al., 2017; Friedl and Wüest, 2002; Humborg et al., 2000; Maavara et al., 2015; Syvitski et al., 2005; Teodoru and Wehrli, 2005; Vörösmarty et al., 2003; Walling, 2006). Syvitski et al. (2005) estimated a reduction of the global riverine flux of particulates to the oceans by 1.4 Gt year^{-1} due to retention within reservoirs. The main negative impacts of these trapped particulates mentioned are the reduced storage capacity and thus, the reduced operational time of the reservoirs, as well as coastal retreat due to reduced particulate supply to coastal regions (Bergkamp et al., 2000; Syvitski et al., 2005). Studies exploring the effect of river damming on nutrient dynamics usually consider the dissolved and organic nutrient fluxes and assume that the inorganic particulate flux is not bioavailable. Maavara et al. (2015) for example estimated a global annual P retention for the year 2000 of 42 Gmol from which 18 Gmol was 'reactive phosphorous' and 24 Gmol considered as 'unreactive particulate P', mainly composed of crystalline phosphate-bearing minerals. The results obtained in this study, however, suggest that the inorganic P within particulates may as well be bioavailable and may directly serve as slow release fertilizer for phytoplankton. Besides the reduction of particulate material, dam construction causes notable alterations of nutrient ratios (Friedl and Wüest, 2002; Humborg et al., 2000; Maavara et al., 2015). Whereas the retention of P and N in artificial reservoirs counteracts anthropogenic eutrophication, the retention of Si is believed to cause harmful algae blooms in downstream environments due to changing phytoplankton species distribution (Chen et al., 2017; Humborg et al., 2000). The role of riverine suspended material in buffering nutrient ratios and thus, its effect on algae blooms has yet to be investigated.

Note that the role of riverine particulate material on primary productivity and elemental budgets gets of global importance in marine systems, where RPM are expected to increase primary productivity and enhance organic carbon burial through the delivery of particulate surface area (Jeandel and Oelkers 2015 and references therein). The direct attachment of bacteria on mineral surfaces presented in this study, support this theory. Moreover, the frequent occurrence of cyanobacteria aggregates associated with sediment particles observed in this study (see Figure 13), suggests a positive effect of RPM on the aggregation and settling of cyanobacteria, facilitating organic carbon burial.

6. Conclusions

The results presented in this study demonstrate the positive effect of riverine suspended material on the growth of freshwater cyanobacteria *Synechococcus sp.* Riverine particulates exhibited three distinct effects on bacterial growth, which are 1) they trigger bacterial growth in otherwise unfavourable growth conditions (e.g. by increasing pH), 2) they increasing maximum total biomass concentration, and 3) their presence induces steady bacterial growth in post-exponential growth phase. These effects are favoured by increasing particulate concentration. Results furthermore suggest a positive feedback between particulates and growing bacteria, where dissolving particulates enhance bacterial growth, which in turn enhances silicate mineral dissolution by altering fluid pH. SEM images showed direct physical contact between particulates and cyanobacteria through organic fibres, suggesting that bacteria attach on mineral surfaces to gain required nutrients. Furthermore, frequent bacteria clusters were observed associated with particulates, suggesting an increasing accumulation of bacteria in the presence of particulate material.

These results indicate a notable influence of riverine particulate material on phytoplankton growth in freshwater environments. However, its potential effect on natural systems requires a case-by-case study depending on various environmental factors such as nutrient availability and nutrient ratios, light intensity or phytoplankton species distribution. Given the predominance of potentially limiting nutrients transported in riverine particulates compared to its dissolved flux, it seems likely that particulates enhance bacterial growth whenever growth is limited by nutrient availability. Furthermore, the direct attachment of bacteria on mineral surfaces underscores the importance of riverine particulates on the burial efficiency of organic carbon. These effects combined suggest a significant impact of particulate material on the global carbon cycle.

Acknowledgements

This research was supported by the Marie Curie EU-FP7 CO2-REACT Research and Training Network. OP acknowledges partial support from RFBR projects Nos 19-55-15002 and 17-05-00348. The authors would like to thank Liudmila Shirokova, Carole Causserand, Aurélie Lanzanova, Frédéric Candaudap and Michel Thibaut from the Géosciences Environnement Toulouse for their help with experimental work, wet chemical analyses, and XRD- measurements, respectively. Stefanie Lutz, Maren Kahl, Martin Fuller and Richard Walshaw from the School of Earth and Environment, University of Leeds are acknowledged for their help with SEM investigations. Eydis Eiriksdottir, Deirdre Clark, Rebecca Neely and

Sigurdur Gislason from the Earth Science Department of the University of Iceland are acknowledged for the provision of suspended particulate material and for support during field work. Sigrid Hirth-Walther, Sebastian Weber and Kurt Bucher from the institute of Geo- und Umweltnaturwissenschaften, Albert-Ludwigs Universität, are likewise acknowledged for their cooperation and help during this study. The authors deeply thank two anonymous reviewers for their fruitful comments.

References

Alley, R.B., Cuffey, K.M., Evenson, E.B., Strasser, J.C., Lawson, D.E., Larson, G.J., 1997. How glaciers entrain and transport basal sediment: Physical constraints. Quaternary Sci. Rev. 16 (9), 1017–1038. doi:10.1016/S0277-3791(97)00034-6.

Anderson, D.M., Glibert, P.M., Burkholder, J.M., 2002. Harmful algal blooms and eutrophication: Nutrient sources, composition, and consequences. Estuaries 25 (4), 704–726. doi:10.1007/BF02804901.

Bailey, B., Templeton, A., Staudigel, H., Tebo, B.M., 2009. Utilization of Substrate Components during Basaltic Glass Colonization by Pseudomonas and Shewanella Isolates. Geomicrobiol. J. 26 (8), 648–656. doi:10.1080/01490450903263376.

Baisre, J.A., Arboleya, Z., 2006. Going against the flow: Effects of river damming in Cuban fisheries. Fish. Res. 81 (2), 283–292. doi:10.1016/j.fishres.2006.04.019.

Bennett, P.C., Rogers, J.R., Choi, W.J., Hiebert, F.K., 2001. Silicates, Silicate Weathering, and Microbial Ecology. Geomicrobiol. J. 18 (1), 3–19. doi:10.1080/01490450151079734.

Bergkamp, G., McCartney, M., Dugan, P., McNeely, J., Acreman, M., 2000. Dams, ecosystem functions and environmental restoration. WCD Thematic Review Environmental Issues II.1, prepared as an input to the World Commission on Dams, Capetown, www.dams.org.

Berner, R.A., 1982. Burial of organic carbon and pyrite sulfur in the modern ocean: Its geochemical and environmental significance. Am. J. Sci. 282, 451–473. doi:10.2475/ajs.282.4.451.

Berner, R.A., Kothavala, Z., 2001. Geocarb III: A Revised Model of Atmospheric CO_2 over Phanerozoic Time. Am. J. Sci. 301 (2), 182–204. doi:10.2475/ajs.301.2.182.

Berner, R.A., Lasaga, A.C., Garrels, R.M., 1983. The carbonate-silicate geochemical cycle and its effect on atmospheric carbon dioxide over the past 100 million years. Am. J. Sci. 283 (7), 641–683. doi:10.2475/ajs.283.7.641.

Bonneville, S., Morgan, D.J., Schmalenberger, A., Bray, A., Brown, A., Banwart, S.A., Benning, L.G., 2011. Tree-mycorrhiza symbiosis accelerate mineral weathering: Evidences from nanometer-scale elemental fluxes at the hypha–mineral interface. Geochim. Cosmochim. Acta 75 (22), 6988–7005. doi:10.1016/j.gca.2011.08.041.

Broecker, W.S., 1982. Glacial to interglacial changes in ocean chemistry. Prog. Oceanogr. 11 (2), 151–197. doi:10.1016/0079-6611(82)90007-6.

Bundeleva, I.A., Ménez, B., Augé, T., Bodénan, F., Recham, N., Guyot, F., 2014. Effect of cyanobacteria Synechococcus PCC 7942 on carbonation kinetics of olivine at 20°C. Miner. Eng. 59, 2–11. doi:10.1016/j.mineng.2014.01.019.

Burdige, D.J., 2007. Preservation of Organic Matter in Marine Sediments: Controls, Mechanisms, and an Imbalance in Sediment Organic Carbon Budgets? Chem. Rev. 107 (2), 467–485. doi:10.1021/cr050347q.

Chen, C., Mao, Z., Tang, F., Han, G., Jiang, Y., 2017. Declining riverine sediment input impact on spring phytoplankton bloom off the Yangtze River Estuary from 17-year satellite observation. Cont. Shelf. Res. 135, 86–91. doi:10.1016/j.csr.2017.01.012.

Dale, A.W., Nickelsen, L., Scholz, F., Hensen, C., Oschlies, A., Wallmann, K., 2015. A revised global estimate of dissolved iron fluxes from marine sediments. Global Biogeochem. Cycles 29 (5), 691–707. doi:10.1002/2014GB005017.

Dittrich, M., Müller, B., Mavrocordatos, D., Wehrli, B., 2003. Induced Calcite Precipitation by Cyanobacterium Synechococcus. Acta hydrochim. hydrobiol. 31 (2), 162–169. doi:10.1002/aheh.200300486.

Dittrich, M., Sibler, S., 2006. Influence of H^+ and Calcium Ions on Surface Functional Groups of Synechococcus PCC 7942 Cells. Langmuir 22 (12), 5435–5442. doi:10.1021/la0531143.

Drever, J.I., Stillings, L.L., 1997. The role of organic acids in mineral weathering. Colloid. Surface A 120 (1), 167–181. doi:10.1016/S0927-7757(96)03720-X.

Eiriksdottir, E.S., 2016. Weathering and riverine fluxes in pristine and controlled river catchments. PhD Dissertation, Faculty of Earth Sciences, University of Iceland.

Eiriksdottir, E.S., Gislason, S.R., Oelkers, E.H., 2015. Direct evidence of the feedback between climate and nutrient, major, and trace element transport to the oceans. Geochim. Cosmochim. Acta 166, 249–266. doi:10.1016/j.gca.2015.06.005.

Eiriksdottir, E.S., Louvat, P., Gislason, S.R., Óskarsson, N., Hardardóttir, J., 2008. Temporal variation of chemical and mechanical weathering in NE Iceland: Evaluation of a steady-state model of erosion. Earth Planet. Sci. Lett. 272 (1), 78–88. doi:10.1016/j.epsl.2008.04.005.

Eiriksdottir, E.S., Oelkers, E.H., Hardardottir, J., Gislason, S.R., 2017. The impact of damming on riverine fluxes to the ocean: A case study from Eastern Iceland. Water Res. 113, 124–138. doi:10.1016/j.watres.2016.12.029.

Elrod, V.A., Berelson, W.M., Coale, K.H., Johnson, K.S., 2004. The flux of iron from continental shelf sediments: A missing source for global budgets. Geophys. Res. Lett. 31 (12), L12307. doi:10.1029/2004GL020216.

Ernst, A., Deicher, M., Herman, P.M.J., Wollenzien, U.I.A., 2005. Nitrate and Phosphate Affect Cultivability of Cyanobacteria from Environments with Low Nutrient Levels. Appl. Environ. Microb. 71 (6), 3379–3383. doi:10.1128/AEM.71.6.3379-3383.2005.

Falkowski, P.G., 2014. 10.5 - Biogeochemistry of Primary Production, in: Holland, H.D., Turekian, K.K. (Eds.), Treatise on Geochemistry (Second Edition). Elsevier, Oxford, pp. 163–187.

Falkowski, P.G., Barber, R.T., Smetacek, V., 1998. Biogeochemical Controls and Feedbacks on Ocean Primary Production. Science 281 (5374), 200–206. doi:10.1126/science.281.5374.200.

Friedl, G., Wüest, A., 2002. Disrupting biogeochemical cycles - Consequences of damming. Aquat. Sci. 64 (1), 55–65. doi:10.1007/s00027-002-8054-0.

Gaillardet, J., Dupré, B., Allègre, C.J., 1999. Geochemistry of large river suspended sediments: Silicate weathering or recycling tracer? Geochim. Cosmochim. Acta 63 (23), 4037–4051. doi:10.1016/S0016-7037(99)00307-5.

Gaillardet, J., Viers, J., Dupré, B., 2003. 5.09 - Trace Elements in River Waters, in: Holland, H.D., Turekian, K.K. (Eds.), Treatise on Geochemistry. Pergamon, Oxford, pp. 225–272.

Gedney, N., Cox, P.M., Betts, R.A., Boucher, O., Huntingford, C., Stott, P.A., 2006. Detection of a direct carbon dioxide effect in continental river runoff records. Nature 439, 835–838. doi:10.1038/nature04504.

Gislason, S.R., Oelkers, E.H., 2003. Mechanism, rates, and consequences of basaltic glass dissolution: II. An experimental study of the dissolution rates of basaltic glass as a

function of pH and temperature. Geochim. Cosmochim. Acta 67 (20), 3817–3832. doi:10.1016/S0016-7037(03)00176-5.

Gislason, S.R., Oelkers, E.H., Eiriksdottir, E.S., Kardjilov, M.I., Gisladottir, G., Sigfusson, B., Snorrason, A., Elefsen, S., Hardardottir, J., Torssander, P., Oskarsson, N., 2009. Direct evidence of the feedback between climate and weathering. Earth Planet. Sci. Lett. 277 (1), 213–222. doi:10.1016/j.epsl.2008.10.018.

Gislason, S.R., Oelkers, E.H., Snorrason, Á., 2006. Role of river-suspended material in the global carbon cycle. Geology 34 (1), 49–52. doi:10.1130/G22045.1.

Hall, B.G., Acar, H., Nandipati, A., Barlow, M., 2014. Growth Rates Made Easy. Mol. Biol. Evol. 31 (1), 232–238. doi:10.1093/molbev/mst187.

Hodell, D.A., Schelske, C.L., Fahnenstiel, G.L., Robbins, L.L., 1998. Biologically induced calcite and its isotopic composition in Lake Ontario. Limnol. Oceanogr. 43 (2), 187–199. doi:10.4319/lo.1998.43.2.0187.

Humborg, C., Conley, D.J., Rahm, L., Wulff, F., Cociasu, A., Ittekkot, V., 2000. Silicon Retention in River Basins: Far-reaching Effects on Biogeochemistry and Aquatic Food Webs in Coastal Marine Environments. AMBIO: A Journal of the Human Environment 29 (1), 45–50. doi:10.1579/0044-7447-29.1.45.

Jeandel, C., Oelkers, E.H., 2015. The influence of terrigenous particulate material dissolution on ocean chemistry and global element cycles. Chem. Geol. 395, 50–66. doi:10.1016/j.chemgeo.2014.12.001.

Jiang, Z., Liu, J., Chen, J., Chen, Q., Yan, X., Xuan, J., Zeng, J., 2014. Responses of summer phytoplankton community to drastic environmental changes in the Changjiang (Yangtze River) estuary during the past 50 years. Water Res. 54, 1–11. doi:10.1016/j.watres.2014.01.032.

Jickells, T.D., An, Z.S., Andersen, K.K., Baker, A.R., Bergametti, G., Brooks, N., Cao, J.J., Boyd, P.W., Duce, R.A., Hunter, K.A., Kawahata, H., Kubilay, N., laRoche, J., Liss, P.S., Mahowald, N., Prospero, J.M., Ridgwell, A.J., Tegen, I., Torres, R., 2005. Global Iron Connections Between Desert Dust, Ocean Biogeochemistry, and Climate. Science 308 (5718), 67–71. doi:10.1126/science.1105959.

Jones, M.E., Beckler, J.S., Taillefert, M., 2011. The flux of soluble organic-iron(III) complexes from sediments represents a source of stable iron(III) to estuarine waters and to the continental shelf. Limnol. Oceanogr. 56 (5), 1811–1823. doi:10.4319/lo.2011.56.5.1811.

Jones, M.T., Gislason, S.R., 2008. Rapid releases of metal salts and nutrients following the deposition of volcanic ash into aqueous environments. Geochim. Cosmochim. Acta 72 (15), 3661–3680. doi:10.1016/j.gca.2008.05.030.

Jones, M.T., Pearce, C.R., Jeandel, C., Gislason, S.R., Eiriksdottir, E.S., Mavromatis, V., Oelkers, E.H., 2012. Riverine particulate material dissolution as a significant flux of strontium to the oceans. Earth Planet. Sci. Lett. 355-356, 51–59. doi:10.1016/j.epsl.2012.08.040.

Kennedy, M.J., Pevear, D.R., Hill, R.J., 2002. Mineral Surface Control of Organic Carbon in Black Shale. Science 295 (5555), 657. doi:10.1126/science.1066611.

Labat, D., Goddéris, Y., Probst, J.L., Guyot, J.L., 2004. Evidence for global runoff increase related to climate warming. Adv. Water Resour. 27 (6), 631–642. doi:10.1016/j.advwatres.2004.02.020.

Lalonde, K., Mucci, A., Ouellet, A., Gélinas, Y., 2012. Preservation of organic matter in sediments promoted by iron. Nature 483 (7388), 198–200. doi:10.1038/nature10855.

Lee, B.D., Apel, W.A., Walton, M.R., 2006. Calcium carbonate formation by Synechococcus sp. strain PCC 8806 and Synechococcus sp. strain PCC 8807. Bioressource Technol. 97 (18), 2427–2434. doi:10.1016/j.biortech.2005.09.028.

Maavara, T., Parsons, C.T., Ridenour, C., Stojanovic, S., Dürr, H.H., Powley, H.R., van Cappellen, P., 2015. Global phosphorus retention by river damming. P. Natl. Acad. Sci. USA 112 (51), 15603–15608. doi:10.1073/pnas.1511797112.

Mayer, L.M., 1994. Surface area control of organic carbon accumulation in continental shelf sediments. Geochim. Cosmochim. Acta 58 (4), 1271–1284. doi:10.1016/0016-7037(94)90381-6.

Meybeck, M., Laroche, L., Dürr, H.H., Syvitski, J.P.M., 2003. Global variability of daily total suspended solids and their fluxes in rivers. Global and Planet. Change 39 (1), 65–93. doi:10.1016/S0921-8181(03)00018-3.

Milliman, J.D., Syvitski, J.P.M., 1992. Geomorphic/Tectonic Control of Sediment Discharge to the Ocean: The Importance of Small Mountainous Rivers. J. Geol. 100 (5), 525–544. doi:10.1086/629606.

Mills, M.M., Ridame, C., Davey, M., La Roche, J., Geider, R.J., 2004. Iron and phosphorus co-limit nitrogen fixation in the eastern tropical North Atlantic. Nature 429, 292-294. doi:10.1038/nature02550.

Obst, M., Dynes, J.J., Lawrence, J.R., Swerhone, G.D.W., Benzerara, K., Karunakaran, C., Kaznatcheev, K., Tyliszczak, T., Hitchcock, A.P., 2009a. Precipitation of amorphous $CaCO_3$ (aragonite-like) by cyanobacteria: A STXM study of the influence of EPS on the nucleation process. Geochim. Cosmochim. Acta 73 (14), 4180–4198. doi:10.1016/j.gca.2009.04.013.

Obst, M., Wehrli, B., Dittrich, M., 2009b. $CaCO_3$ nucleation by cyanobacteria: Laboratory evidence for a passive, surface-induced mechanism. Geobiology 7 (3), 324–347. doi:10.1111/j.1472-4669.2009.00200.x.

Oelkers, E.H., Benning, L.G., Lutz, S., Mavromatis, V., Pearce, C.R., Plümper, O., 2015. The efficient long-term inhibition of forsterite dissolution by common soil bacteria and fungi at Earth surface conditions. Geochim. Cosmochim. Acta 168, 222–235. doi:10.1016/j.gca.2015.06.004.

Oelkers, E.H., Gislason, S.R., Eiriksdottir, E.S., Jones, M., Pearce, C.R., Jeandel, C., 2011. The role of riverine particulate material on the global cycles of the elements. Appl. Geochem. 26, S365-S369. doi:10.1016/j.apgeochem.2011.03.062.

Oelkers, E.H., Jones, M.T., Pearce, C.R., Jeandel, C., Eiriksdottir, E.S., Gislason, S.R., 2012. Riverine particulate material dissolution in seawater and its implications for the global cycles of the elements. C. R. Geosci. 344 (11), 646–651. doi:10.1016/j.crte.2012.08.005.

Olsson, J., Stipp, S.L., Dalby, K.N., Gislason, S.R., 2013. Rapid release of metal salts and nutrients from the 2011 Grímsvötn, Iceland volcanic ash. Geochim. Cosmochim. Acta 123, 134–149. doi:10.1016/j.gca.2013.09.009.

Olsson-Francis, K., Simpson, A.E., Wolff-Boenisch, D., Cockell, C.S., 2012. The effect of rock composition on cyanobacterial weathering of crystalline basalt and rhyolite. Geobiology 10 (5), 434–444. doi:10.1111/j.1472-4669.2012.00333.x.

Perez, A., Rossano, S., Trcera, N., Huguenot, D., Fourdrin, C., Verney-Carron, A., van Hullebusch, E.D., Guyot, F., 2016. Bioalteration of synthetic Fe(III)-, Fe(II)-bearing basaltic glasses and Fe-free glass in the presence of the heterotrophic bacteria strain Pseudomonas aeruginosa: Impact of siderophores. Geochim. Cosmochim. Acta 188, 147–162. doi:10.1016/j.gca.2016.05.028.

Poulton, S.W., Raiswell, R., 2005. Chemical and physical characteristics of iron oxides in riverine and glacial meltwater sediments. Chem. Geol. 218 (3), 203–221. doi:10.1016/j.chemgeo.2005.01.007.

Radic, A., Lacan, F., Murray, J.W., 2011. Iron isotopes in the seawater of the equatorial Pacific Ocean: New constraints for the oceanic iron cycle. Earth Planet. Sci. Lett. 306 (1), 1–10. doi:10.1016/j.epsl.2011.03.015.

Rippka, R., Deruelles, J., Waterbury, J.B., Herdman, M., Stanier, R.Y., 1979. Generic Assignments, Strain Histories and Properties of Pure Cultures of Cyanobacteria. Microbiology 111 (1), 1–61. doi:10.1099/00221287-111-1-1. http://mic.microbiologyresearch.org/content/journal/micro/10.1099/00221287-111-1-1.

Rogers, J.R., Bennett, P.C., 2004. Mineral stimulation of subsurface microorganisms: Release of limiting nutrients from silicates. Chem. Geol. 203 (1), 91–108. doi:10.1016/j.chemgeo.2003.09.001.

Rogers, J.R., Bennett, P.C., Choi, W.J., 1998. Feldspars as a source of nutrients for microorganisms. Am. Mineral. 83 (11), 1532–1540. doi:10.2138/am-1998-1114.

Rohwer, F., Thurber, R.V., 2009. Viruses manipulate the marine environment. Nature 459 (7244), 207-212. doi:10.1038/nature08060.

SCOR UNESCO, 1966. Determination of photosynthetic pigments in seawater - Report of SCOR-UNESCO Working group 17 (Paris). Mg. Ocean. Methodol. 1.

Smits, M.M., Bonneville, S., Benning, L.G., Banwart, S.A., Leake, J.R., 2012. Plant-driven weathering of apatite – the role of an ectomycorrhizal fungus. Geobiology 10 (5), 445–456. doi:10.1111/j.1472-4669.2012.00331.x.

Stabel, H.-H., 1986. Calcite precipitation in Lake Constance: Chemical equilibrium, sedimentation, and nucleation by algae1. Limnol. Oceanogr. 31 (5), 1081–1094. doi:10.4319/lo.1986.31.5.1081.

Stockmann, G.J., Shirokova, L.S., Pokrovsky, O.S., Bénézeth, P., Bovet, N., Gislason, S.R., Oelkers, E.H., 2012. Does the presence of heterotrophic bacterium Pseudomonas reactans affect basaltic glass dissolution rates? Chem. Geol. 296-297, 1–18. doi:10.1016/j.chemgeo.2011.12.011.

Sudek, L.A., Wanger, G., Templeton, A.S., Staudigel, H., Tebo, B.M., 2017. Submarine Basaltic Glass Colonization by the Heterotrophic Fe(II)-Oxidizing and Siderophore-Producing Deep-Sea Bacterium Pseudomonas stutzeri VS-10: The Potential Role of Basalt in Enhancing Growth. Front. Microbiol. 8, 363. doi:10.3389/fmicb.2017.00363.

Syvitski, J.P.M., Peckham, S.D., Hilberman, R., Mulder, T., 2003. Predicting the terrestrial flux of sediment to the global ocean: A planetary perspective. Sediment. Geol. 162 (1), 5–24. doi:10.1016/S0037-0738(03)00232-X.

Syvitski, J.P.M., Vörösmarty, C.J., Kettner, A.J., Green, P., 2005. Impact of Humans on the Flux of Terrestrial Sediment to the Global Coastal Ocean. Science 308 (5720), 376–380. doi:10.1126/science.1109454.

Teodoru, C., Wehrli, B., 2005. Retention of Sediments and Nutrients in the Iron Gate I Reservoir on the Danube River. Biogeochemistry 76 (3), 539–565. doi:10.1007/s10533-005-0230-6.

Thompson, J.B., Schultze-Lam, S., Beveridge, T.J., Des Marais, D.J., 1997. Whiting events: Biogenic origin due to the photosynthetic activity of cyanobacterial picoplankton. Limnol. Oceanogr. 42 (1), 133–141. doi:10.4319/lo.1997.42.1.0133.

Uroz, S., Calvaruso, C., Turpault, M.-P., Frey-Klett, P., 2009. Mineral weathering by bacteria: Ecology, actors and mechanisms. Trends Microbiol. 17 (8), 378–387. doi:10.1016/j.tim.2009.05.004.

Viers, J., Dupré, B., Gaillardet, J., 2009. Chemical composition of suspended sediments in World Rivers: New insights from a new database. Sci. Total Environ. 407 (2), 853–868. doi:10.1016/j.scitotenv.2008.09.053.

Vörösmarty, C.J., Meybeck, M., Fekete, B., Sharma, K., Green, P., Syvitski, J.P.M., 2003. Anthropogenic sediment retention: Major global impact from registered river impoundments. Global and Planet. Change 39 (1), 169–190. doi:10.1016/S0921-8181(03)00023-7.

Walker, J.C.G., Hays, P.B., Kasting, J.F., 1981. A negative feedback mechanism for the long-term stabilization of Earth's surface temperature. J. Geophys. Res.-Oceans 86 (C10), 9776–9782. doi:10.1029/JC086iC10p09776.

Walling, D.E., 2006. Human impact on land–ocean sediment transfer by the world's rivers. Geomorphology 79 (3), 192–216. doi:10.1016/j.geomorph.2006.06.019.

Wallmann, K., 2001. Controls on the cretaceous and cenozoic evolution of seawater composition, atmospheric CO_2 and climate. Geochim. Cosmochim. Acta 65 (18), 3005–3025. doi:10.1016/S0016-7037(01)00638-X.

Wu, L., Jacobson, A.D., Chen, H.-C., Hausner, M., 2007. Characterization of elemental release during microbe–basalt interactions at T=28°C. Geochim. Cosmochim. Acta 71 (9), 2224–2239. doi:10.1016/j.gca.2007.02.017.

Wu, L., Jacobson, A.D., Hausner, M., 2008. Characterization of elemental release during microbe–granite interactions at T=28°C. Geochim. Cosmochim. Acta 72 (4), 1076–1095. doi:10.1016/j.gca.2007.11.025.

Table A1: Summary of experimental conditions. RPM means Riverine Particulate Material. ICE means Iceland and MS Mississippi particulates.

Experiment ID	Electrolyte BG-11 dilution	type of RPM	RPM mass [mg/kg]	Particual sterilization method	Initial biomass [$g_{(dry)}$/kg]	pH initial	pH max	duration [days]	Parameters measured	displayed in Figure
S*II* 1	13.3%	-	0	-	0.022	Nd	nd	28	OD	
S*II* 2	13.3%	ICE	1505	no sterilization	0.021	Nd	nd	28	OD	
S*II* 3	13.3%	MS	1506	no sterilization	0.022	Nd	nd	28	OD	
S*III* 1	5%	-	0	-	0.032	Nd	nd	36	OD	
S*III* 2	5%	ICE	501	no sterilization	0.033	Nd	nd	36	OD	
S*III* 3	5%	ICE	1503	no sterilization	0.033	Nd	nd	36	OD, SEM	
S*III* 4	5%	MS	498	no sterilization	0.033	Nd	nd	36	OD	
S*III* 5	5%	MS	1498	no sterilization	0.034	Nd	nd	36	OD, SEM	
S*IV* 1	5%	ICE	1501	12h at 121°C	0.007	6.0	9.8	22	OD, pH	
S*IV* 2	5%	ICE	76	12h at 121°C	0.007	6.0	6.3	22	OD, pH	
S*IV* 3	5%	MS	1495	12h at 121°C	0.007	6.0	10.7	22	OD, pH	
S*IV* 4	5%	MS	75	12h at 121°C	0.007	6.0	6.5	22	OD, pH	
S*IV* 5	5%	ICE	1499	12h at 121°C	0	6.0	7.1	22	OD, pH	
S*IV* 6	5%	ICE	75	12h at 121°C	0	6.0	6.2	22	OD, pH	
S*IV* 7	5%	MS	1500	12h at 121°C	0	6.0	7.8	22	OD, pH	
S*IV* 8	5%	MS	76	12h at 121°C	0	6.0	6.6	22	OD, pH	
S*IV* 9	5%	-	0	-	0.007	6.0	6.3	22	OD, pH	
S*V* 1	5%	-	0	-	0.018	6.0	6.6	28	OD, pH, NPOC, DIC, ICP-MS	4, 6, 11, 12
S*V* 2	5%	ICE	1489	10 % H_2O_2	0.018	6.0	10.1	28	OD, pH, NPOC, DIC, ICP-MS	4, 6, 11, 12
S*V* 3	5%	ICE	76	10 % H_2O_2	0.018	6.0	6.5	28	OD, pH, NPOC, DIC, ICP-MS	6
S*V* 4	5%	MS	1501	10 % H_2O_2	0.018	6.0	10.6	28	OD, pH, NPOC, DIC, ICP-MS	4, 6, 11, 12
S*V* 5	5%	MS	76	10 % H_2O_2	0.018	6.0	6.9	28	OD, pH, NPOC, DIC, ICP-MS	6
S*V* 6	5%	ICE	1495	10 % H_2O_2	0	6.0	6.9	28	OD, pH, NPOC, DIC, ICP-MS	11, 12
S*V* 7	5%	ICE	77	10 % H_2O_2	0	6.0	6.4	28	OD, pH, NPOC, DIC, ICP-MS	
S*V* 8	5%	MS	1502	10 % H_2O_2	0	6.0	7.6	28	OD, pH, NPOC, DIC, ICP-MS	11, 12
S*V* 9	5%	MS	75	10 % H_2O_2	0	6.0	6.7	28	OD, pH, NPOC, DIC, ICP-MS	
S*V* 10	5%	-	0	-	0	6.0	6.2	28	OD, pH, NPOC, DIC, ICP-MS	
S*Vb* 1	5%	-	0	-	0.018	Nd		28	OD	4, 6

S*Vb* 7	5%	MS	1524	12h at 121°C	0	Nd	nd	28	OD			
S*VI* 1	5% + NaOH	organic ctrl			0.041	6.8	10.6	28	OD, pH			9
S*VI* 2	5% + NaOH	MS	1499	Eth + 12h 121°C	0.041	6.8	10.8	28	OD, pH			9
S*VI* 3	5% + NaOH	MS	78	Eth + 12h 121°C	0.041	6.8	10.6	28	OD, pH			9
S*VI* 4	5% + NaOH	MS	1501	Eth + 12h 121°C	0	6.8	7.8	28	OD, pH			
S*VI* 5	5% + NaOH	MS	76	Eth + 12h 121°C	0	6.8	7.1	28	OD, pH			
S*VI* 6	5% + NaOH	-	0	-	0	6.8	6.9	28	OD, pH			
S*VI* 7	5% + NaOH	MS	1007	Eth + 12h 121°C	0.041	6.8	nd	28	OD			9
S*VI* 8	5% + NaOH	MS	514	Eth + 12h 121°C	0.041	6.8	nd	28	OD			9
S*VI* 9	5% + NaOH	MS	1005	Eth + 12h 121°C	0.018	6.8	nd	28	OD			
S*VI* 10	5% + NaOH	MS	506	Eth + 12h 121°C	0.018	6.8	nd	28	OD			
S*VI* 11	5% + NaOH	MS	1493	Eth + 12h 121°C	0.007	6.8	nd	28	OD			
S*VI* 12	5% + NaOH	MS	1006	Eth + 12h 121°C	0.007	6.8	nd	28	OD			
S*VI* 13	5% + NaOH	MS	502	Eth + 12h 121°C	0.007	6.8	nd	28	OD			
S*VI* 14	5% + NaOH	MS	1010	Eth + 12h 121°C	0	6.8	nd	28	OD			
S*VI* 15	5% + NaOH	MS	497	Eth + 12h 121°C	0	6.8	nd	28	OD			
S*VI* 16	13.3%	-	0	-	0.030	Nd	nd	28	OD			10
S*VI* 17	13.3%	MS	1487	Eth + 12h 121°C	0.032	Nd	nd	28	OD			10
S*VI* 18	13.3%	MS	1000	Eth + 12h 121°C	0.030	Nd	nd	28	OD			10
S*VI* 19	13.3%	MS	508	Eth + 12h 121°C	0.030	Nd	nd	28	OD			10
S*VI* 20	13.3%	MS	74	Eth + 12h 121°C	0.030	Nd	nd	28	OD			10
S*VII* 1	5% + NaOH	-	0	-	0.007	7.4	9.4	27	OD, pH, Cond			
S*VII* 2	5% + NaOH	-	0	-	0.018	7.6	9.7	27	OD, pH, Cond			
S*VII* 3	5% + NaOH	-	0	-	0.041	7.6	10.1	27	OD, pH, Cond		7	
S*VII* 4	5% + 0.3g/kg NaCl	-	0	-	0.007	6.0	6.3	27	OD, pH, Cond			
S*VII* 5	5% + 0.3g/kg NaCl	-	0	-	0.018	6.0	6.3	27	OD, pH, Cond			
S*VII* 6	5% + 0.3g/kg NaCl	-	0	-	0.041	6.0	6.5	27	OD, pH, Cond		7	
S*VII* 7	5% + HCO_3/Ca	-	0	-	0.007	7.6	9.9	27	OD, pH, Cond			
S*VII* 8	5% + HCO_3/Ca	-	0	-	0.018	7.6	10.4	27	OD, pH, Cond			
S*VII* 9	5% + HCO3/Ca	-	0	-	0.041	7.8	10.6	27	OD, pH, Cond		7	
S*VII* 10	5%	-	0	-	0.007	6.1	6.6	27	OD, pH, Cond	5		
S*VII* 11	5%	-	0	-	0.018	6.1	6.5	27	OD, pH, Cond	4, 5		
S*VII* 12	5%	-	0	-	0.041	6.0	6.6	27	OD, pH, Cond, Chl a	5,	7,	9
S*VII* 13	5%	MS	1543	Eth + 12h 121°C	0.007	6.0	10.3	27	OD, pH, Cond	5		
S*VII* 14	5%	MS	1509	Eth + 12h 121°C	0.018	5.9	10.3	27	OD, pH, Cond	4, 5		
S*VII* 15	5%	MS	1541	Eth + 12h 121°C	0.041	5.9	10.5	27	OD, pH, Cond, Chl a	5,	7,	9
S*VII* 16	5%	MS	1001	Eth + 12h 121°C	0.007	Nd	nd	27	OD			
S*VII* 17	5%	MS	1474	burned	0.007	Nd	nd	27	OD			
S*VII* 18	5%	MS	1458	burned	0.018	Nd	nd	27	OD	4		
S*VII* 19	5%	MS	1497	burned	0.041	Nd	nd	27	OD			
S*VII* 20	5%	Zircon	1452	Eth + 12h 121°C	0.007	Nd	nd	13	OD			

S*VII* 21	5%	Zircon	1497	Eth + 12h 121°C	0.041	Nd	nd	13	OD	7
S*VII* 22	5%	MS	1477	Eth + 12h 121°C	0	5.9	7.7	19	OD, pH	
S*VII* 23	5%	MS	994	Eth + 12h 121°C	0.041	Nd	nd	27	OD, pH, Cond	7, 9
S*VII* 24	5%	MS	508	Eth + 12h 121°C	0.041	Nd	nd	27	OD, Chl a	9
S*VII* 25	5%	MS	70	Eth + 12h 121°C	0.041	Nd	nd	28	OD	9
S*VIII* 1	5% + NaOH	-	0	-	0.007	7.1	9.5	27	OD, pH	
S*VIII* 2	5% + NaOH	-	0	-	0.018	7.1	9.5	27	OD, pH	
S*VIII* 3	5% + NaOH	-	0	-	0.041	7.1	10.5	27	OD, pH	
S*VIII* 4	5%	MS	1007	Eth + 12h 121°C	0.041	6.1	10.1	27	OD, pH	
S*VIII* 5	5%	-	0	-	0.041	6.1	6.2	12	OD, pH	
S*VIII* 6	5%	-	0	-	0.041	6.1	6.2	12	OD, pH	
S*IX* 1	5% + carb buff.	-	0	-	0.007	9.4	9.6	24	OD, pH	8
S*IX* 2	5% + carb buff.	-	0	-	0.018	9.4	9.7	24	OD, pH	8
S*IX* 3	5% + carb buff.	MS	512	Eth + 12h 121°C	0.007	9.4	9.8	24	OD, pH	8
S*IX* 4	5% + carb buff.	MS	526	Eth + 12h 121°C	0.018	9.4	9.6	24	OD, pH	8
S*X* 1	5%	-	0	-	0.007	5.8	6.2	15	OD, pH, Cond	5
S*X* 2	5%	ICE	1497	Eth + 12h 121°C	0.007	6.6	10.0	15	OD, pH, Cond	
S*X* 3	5%	-	0	-	0.018	5.8	6.4	15	OD, pH, Cond	4
S*X* 4	5%	ICE	1482	Eth + 12h 121°C	0.018	6.4	10.0	15	OD, pH, Cond	4, 5
S*X* 5	5%	-	0	-	0.041	5.8	6.5	15	OD, pH, Cond, Chl a	
S*X* 6	5%	ICE	81	Eth + 12h 121°C	0.041	Nd	nd	15	OD	5
S*X* 7	5%	ICE	1504	Eth + 12h 121°C	0.041	6.9	10.4	15	OD, pH, Cond Chl a	5
S*X* 8	5%	ICE	1478	Eth + 12h 121°C	0	6.6	7.0	15	OD, pH, Cond	
S*X* 9	5%	ICE	1468	burned	0.018	Nd	nd	15	OD	4, 5
S*X* 10	5% + NaOH	-	0	-	0.041	7.1	9.9	25	OD, pH	5
S*X* 11	5% + NaOH	-	0	-	0.018	7.2	9.7	25	OD, pH	
S*X* 12	5%	MS	1464	Eth + 12h 121°C	0	6.2	7.6	25	OD, pH, Cond	
S*X* 13	5%	MS	1531	Eth + 12h 121°C	0.007	Nd	nd	25	OD	
S*X* 14	5%	MS	505	Eth + 12h 121°C	0.007	Nd	nd	25	OD	

Table A 2: Initial conditions, maximal biomass concentration and computed growth rate constants in exponential (μ) and in stationary phase (μ_{stat}) for all reactors.

Experiment ID	RPM [mg/kg]	type of RPM	biomass initial [$g_{(dry)}$/kg]	pH initial	pH max	max biomass [$g_{(dry)}$/kg]	Growth rate constant μ [$days^{-1}$]	± [$days^{-1}$]	Slope in stat. phase μ_{stat} [$g_{(dry)}$/kg/day]	± [$g_{(dry)}$/kg/day]	displayed in figure
S*II* 1	0		0.022	nd	nd	0.267	0.431	0.010	-9.75E-04	7.62E-04	
S*II* 2	1505	ICE	0.021	nd	nd	0.343	0.476	0.095	3.35E-03	7.33E-04	
S*II* 3	1506	MS	0.022	nd	nd	0.368	0.435	0.096	4.30E-03	2.93E-04	
S*III* 1	0		0.032	nd	nd	0.115	0.466	0.093	1.80E-04	5.70E-05	
S*III* 2	501	ICE	0.033	nd	nd	0.141	0.395	0.008	2.17E-04	7.32E-05	
S*III* 3	1503	ICE	0.033	nd	nd	0.157	0.431	0.062	-2.92E-04	1.24E-04	
S*III* 4	498	MS	0.033	nd	nd	0.153	0.388	0.127	8.18E-04	6.19E-05	
S*III* 5	1498	MS	0.034	nd	nd	0.219	0.382	0.010	2.68E-03	1.01E-04	
S*IV* 1	1501	ICE	0.007	6.0	9.8	0.133	0.390	0.007	6.92E-04	6.54E-05	
S*IV* 2	76	ICE	0.007	6.0	6.3			no growth			
S*IV* 3	1495	MS	0.007	6.0	10.7	0.140	0.465	0.038	1.59E-03	2.91E-04	
S*IV* 4	75	MS	0.007	6.0	6.5			no growth			
S*IV* 9	0		0.007	6.0	6.3			no growth			
S*V* 1	0		0.018	6.0	6.6			no growth			4, 6, 11, 12
S*V* 2	1489	ICE	0.018	6.0	10.1	0.134	0.274	0.005	-1.69E-04	1.62E-04	4, 6, 11, 12
S*V* 3	76	ICE	0.018	6.0	6.5			no growth			6
S*V* 4	1501	MS	0.018	6.0	10.6	0.142	0.301	0.001	#BEZUG!	5.03E-05	4, 6, 11, 12
S*V* 5	76	MS	0.018	6.0	6.9			no growth			6
S*Vb* 1	0		0.018	nd				no growth			4, 6
S*Vb* 2	1517	ICE	0.018	nd	nd	0.157	0.348	0.011	-3.74E-05	4.26E-05	4, 6
S*Vb* 3	Residual S*V* 6		0.018	6.8	nd	0.067	0.234	0.012	-1.54E-04	4.05E-05	6
S*Vb* 4	1506	MS	0.018	nd	nd	0.159	0.483	0.018	1.06E-03	5.17E-05	4, 6
S*Vb* 5	Residual S*V* 8		0.018	7.6	nd	0.080	0.255	0.007	-1.24E-04	4.04E-05	6
S*VI* 1	0		0.041	6.8	10.6	0.135	0.209	0.005	-7.99E-04	1.64E-04	9
S*VI* 2	1499	MS	0.041	6.8	10.8	0.178	0.228	0.019	1.12E-03	1.06E-04	9
S*VI* 3	78	MS	0.041	6.8	10.6	0.142	0.215	0.013	-4.11E-04	1.03E-04	9
S*VI* 7	1007	MS	0.041	6.8	nd	0.161	0.253	0.005	4.28E-05	6.35E-05	9
S*VI* 8	514	MS	0.041	6.8	nd	0.157	0.240	0.010	-6.84E-05	5.88E-05	9
S*VI* 9	1005	MS	0.018	6.8	nd	0.147	0.346	0.009	4.23E-04	7.70E-05	
S*VI* 10	506	MS	0.018	6.8	nd	0.134	0.355	0.021	-2.54E-05	5.35E-05	
S*VI* 11	1493	MS	0.007	6.8	nd	0.142	0.473	0.003	8.48E-04	7.09E-05	

S*VI* 12	1006	MS	0.007	6.8	nd	0.167	0.399	0.011	-2.48E-04	8.50E-05			
S*VI* 13	502	MS	0.007	6.8	nd	0.120	0.403	0.012	-1.88E-05	7.32E-05			
S*VI* 16	0		0.030	nd	nd	0.286	0.310	0.012					10
S*VI* 17	1487	MS	0.032	nd	nd	0.346	0.309	0.005		1.24E-04			10
S*VI* 18	1000	MS	0.030	nd	nd	0.33	0.301	0.017		2.04E-04			10
S*VI* 19	508	MS	0.030	nd	nd	0.327	0.283	0.009		1.63E-04			10
S*VI* 20	74	MS	0.030	nd	nd	0.303	0.291	0.009		2.15E-04			10
S*VII* 1	0		0.007	7.4	9.4	0.081	0.410	0.043	-1.27E-03	4.78E-05			
S*VII* 2	0		0.018	7.6	9.7	0.099	0.347	0.020	-1.06E-03	7.09E-05			
S*VII* 3	0		0.041	7.6	10.1	0.128	0.230	0.026	-1.39E-03	5.25E-05		7	
S*VII* 4	0		0.007	6.0	6.3			no growth					
S*VII* 5	0		0.018	6.0	6.3			no growth					
S*VII* 6	0		0.041	6.0	6.5			no growth				7	
S*VII* 7	0		0.007	7.6	9.9	0.107	0.591	0.107	-6.68E-04	1.18E-04			
S*VII* 8	0		0.018	7.6	10.4	0.125	0.411	0.020	-9.53E-04	2.35E-05			
S*VII* 9	0		0.041	7.8	10.6	0.160	0.300	0.021	-1.55E-03	1.21E-04		7	
S*VII* 10	0		0.007	6.1	6.6			no growth			5		
S*VII* 11	0		0.018	6.1	6.5			no growth			4, 5		
S*VII* 12	0		0.041	6.0	6.6			no growth			5,	7,	9
S*VII* 13	1543	MS	0.007	6.0	10.3	0.143	0.505	0.022	1.05E-03	1.48E-04	5		
S*VII* 14	1509	MS	0.018	5.9	10.3	0.156	0.409	0.020	9.14E-04	1.19E-04	4, 5		
S*VII* 15	1541	MS	0.041	5.9	10.5	0.197	0.322	0.045	1.42E-03	1.47E-04	5,	7,	9
S*VII* 16	1001	MS	0.007	nd	nd	0.136	0.531	0.012	6.98E-04	1.39E-04			
S*VII* 17	1474	MS	0.007	nd	nd	0.137	0.526	0.027	8.51E-04	1.61E-04			
S*VII* 18	1458	MS	0.018	nd	nd	0.148	0.446	0.019	5.46E-04	6.21E-05	4		
S*VII* 19	1497	MS	0.041	nd	nd	0.171	0.390	0.078	2.85E-04	8.37E-05			
S*VII* 20	1452	Zircone	0.007	nd	nd			no growth					
S*VII* 21	1497	Zircone	0.041	nd	nd			no growth				7	
S*VII* 23	994	MS	0.041	nd	nd	0.176	0.338	0.047	5.76E-04	6.94E-05		7,	9
S*VII* 24	508	MS	0.041	nd	nd	0.164	0.292	0.019	-1.07E-03	1.66E-04			9
S*VII* 25	70	MS	0.041	nd	nd	0.140	0.271	0.022					9
S*VIII* 1	0		0.007	7.1	9.5	0.084	0.512	0.102	-3.42E-04	8.91E-05			
S*VIII* 2	0		0.018	7.1	9.5	0.093	0.326	0.065	-4.28E-04	5.18E-05			
S*VIII* 3	0		0.041	7.1	10.5	0.155	0.198	0.040	-1.00E-03	1.01E-04			
S*VIII* 4	1007	MS	0.041	6.1	10.1	0.157	0.411	0.082	3.66E-04	1.69E-04			
S*VIII* 5	0		0.041	6.1	6.2			no growth					
S*VIII* 6	0		0.041	6.1	6.2			no growth					
S*IX* 1	0		0.007	9.4	9.6	0.104	0.532	0.023	-2.33E-03	1.20E-04		8	
S*IX* 2	0		0.018	9.4	9.7	0.112	0.434	0.036	-2.44E-03	1.36E-04		8	
S*IX* 3	512	MS	0.007	9.4	9.8	0.116	0.527	0.049	-2.05E-03	1.49E-04		8	

S*IX* 4	526	MS	0.018	9.4	9.6	0.134	0.467	0.015	-2.37E-03	5.51E-05		8
S*X* 1	0		0.007	5.8	6.2			no growth			5	
S*X* 2	1497	ICE	0.007	6.6	10.0	0.143	0.470	0.018				
S*X* 3	0		0.018	5.8	6.4			no growth			4	
S*X* 4	1482	ICE	0.018	6.4	10.0	0.154	0.405	0.081			4, 5	
S*X* 5	0		0.041	5.8	6.5			no growth				
S*X* 6	81	ICE	0.041	nd	nd			no growth			5	
S*X* 7	1504	ICE	0.041	6.9	10.4	0.186	0.361	0.072			5	
S*X* 9	1468	ICE	0.018	nd	nd	0.159	0.465	0.093			4, 5	
S*X* 10	0		0.041	7.1	9.9	0.139	0.304	0.061	-1.43E-03	8.32E-05	5	
S*X* 11	0		0.018	7.2	9.7	0.113	0.472	0.094	-1.17E-03	8.25E-05		
S*X* 13	1531	MS	0.007	nd	nd	0.135	0.566	0.042	6.69E-04	8.77E-05		
S*X* 14	505	MS	0.007	nd	nd	0.118	0.462	0.045	1.95E-04	8.70E-05		

1224

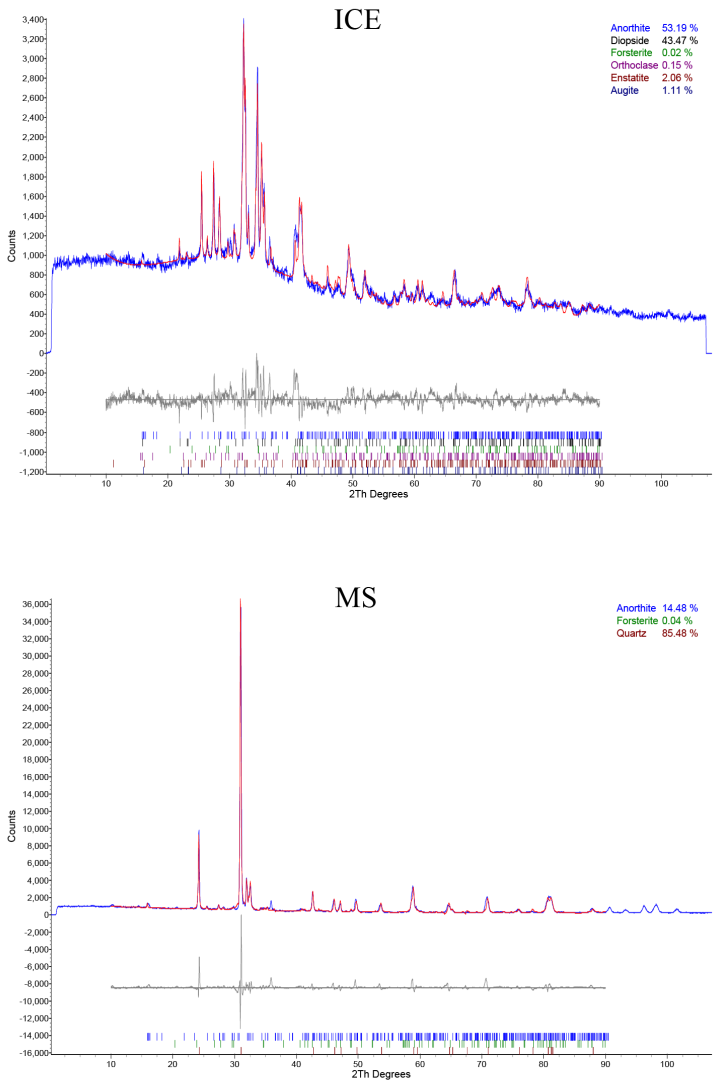

Figure A1: XRD spectra of Iceland (ICE) and Mississippi (MS) riverine particulate material used in this study.

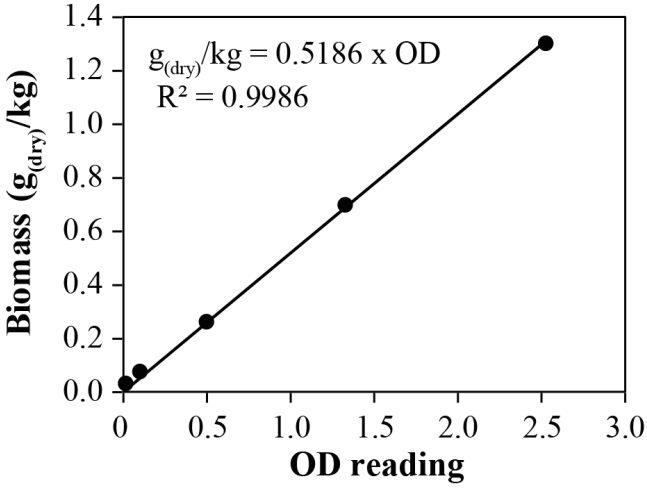

Figure A 2: Optical density (OD) versus biomass ($g_{(dry)}$/kg) calibration curve for determination of biomass concentrations in suspension samples. For OD readings >1, samples were diluted.